



ISAS - INTERNATIONAL SCHOOL FOR ADVANCED STUDIES

THESIS FOR THE ATTAINMENT OF THE TITLE OF

"DOCTOR PHILOSOPHIAE"

MULTIPLE PARTON INTERACTIONS IN HIGH P_T HADRONIC PROCESSES

Candidate:

Dr. Mustapha MEKHFI

Supervisor:

Prof. Nello PAVIER

Academic Year: 1983/84

**SISSA - SCUOLA
INTERNAZIONALE
SUPERIORE
DI STUDI AVANZATI**

TRIESTE
Strada Costiera 11

TRIESTE

To my mother
and all my family.

CONTENTS

=====

- I) INTRODUCTION
- II) MULTIPARTON PROCESSES: PHENOMENOLOGY
 - A) Multi-constituent-scattering as a model for elastic scattering at wide angle
 - A1 - Introduction
 - A2 - Description of the multiparton scattering
 - a) Lowest order QCD results
 - b) Higher order corrections to multiparton scattering in exclusive processes
 - B) Production of baryons with large transverse momenta via the multiple scattering mechanism
 - B1 - Introduction
 - B2 - Description of the model
 - C) Multiparton scattering and large- P_T jet production in hadronic collisions at collider and tevatron energies
 - C1 - Introduction
 - C2 - General considerations on power behaviour of the cross sections
 - C3 - The large- P_T multijet cross section formulae
 - C4 - Numerical estimates
 - D) Production of gauge boson pairs at collider and tevatron energies
 - E) Single and double Drell-Yan mechanism: phenomenological considerations
 - E1 - Single Drell-Yan process in the parton model
 - E2 - Single Drell-Yan process in QCD
 - E3 - QCD phenomenology of single lepton-pair production
 - E4 - Diagrammatic analysis of the first order (α_s) contributions in the (LLA) to the single Drell-Yan process
 - E5 - The double Drell-Yan annihilation: phenomenology

III) THE DOUBLE DRELL-YAN ANNIHILATION: CONCEPTUAL CONSIDERATIONS

\tilde{A}) Formalism of the double scattering

- a) The spin structure of the cut amplitude $\Gamma_{\alpha_1 \beta_1 \alpha_2 \beta_2}$
- b) The colour structure of the cut amplitude $\Gamma_{i_1 j_1 i_2 j_2}$

\tilde{B}) Application to the double Drell-Yan process

- a) Limited phase space of the connecting gluons in double Drell-Yan mechanism
- b) The double Drell-Yan cross-section formula

\tilde{C}) The evolution equation of the structure functions

IV) CONCLUSION

V) APPENDIX

VI) REFERENCES

ACKNOWLEDGEMENTS

This thesis is based on the work done both in Trieste (Italy) and at Orsay (France) with the continuous help of my supervisor, Prof. N. Paver and that of X. Artru and W. Furmanski. I would like to thank them all for the support and advice given to me.

I am grateful to the SISSA direction for their financial support of the present thesis. My gratitude also goes to Dr. K. Chadan for the warm hospitality offered to me at Orsay, and to all colleagues in Trieste for having provided such a pleasant atmosphere. Finally I would like to thank Mrs. Alex Poretti for patiently typing the manuscript.

I. INTRODUCTION

There is by now an ever increasing experimental evidence which confirms the QCD-parton model picture of high energy and high P_T reaction based on single hard collisions between elementary point-like constituents. The composite hadron structure however allows for a new kind of subprocesses to occur already at the naive parton level, that is multiparton processes. The class of disconnected multiparton processes was first considered sometime ago by Landshoff⁽¹⁾ as a model for a wide-angle elastic hadron-hadron scattering. Their phenomenological consequences appear to be successful. The point was however that higher order QCD corrections⁽²⁾ (virtual gluons only) are believed to introduce, in this case, a Sudakov-like suppression. If one looks at an inclusive single particle or jet cross section where initial and/or final partons are allowed to radiate real gluons in all possible ways compatible with the available phase space, rather than an exclusive one, the unwanted virtual gluon contributions which are responsible for the Sudakov-like suppression are cancelled out by the real gluon contributions. Therefore no Sudakov suppression is expected to hold. Thus high P_T physics offers the opportunity to test, in principle the multiscattering mechanism.

Multiple parton processes represent in general, for dimensional reasons power-like corrections^(3,4) to the leading QCD terms. However in some kinematical regions the correct scale parameter for the suppression factor turns out to be not the C.M. energy \sqrt{s} (in which case they would be totally negligible at Collider energies) but rather E_T (for multijet cross section E_T stands for the jet total transverse energy). They provide thus corrections to the leading QCD terms of the form $(\frac{1}{E_T})^p$. Furthermore, disconnected processes are less suppressed than predicted by the naive counting rules⁽⁵⁾ with respect to any connected process involving the same number of constituents. The appearance of E_T as the appropriate scale parameter for the suppression factor rather than

\sqrt{s} in the multijet cross sections has been first pointed out by M. Jacob, reference (6) and shown explicitly in their analysis of the double scattering by N. Paver and D. Treleani, Reference (7) and B. Humpert, reference (8). They conclude that the effect can be observable even at very large C.M. energy provided that E_T is (although large) limited with respect to \sqrt{s} and conversely at fixed E_T , the cross section is expected to increase with increasing \sqrt{s} . The origin of this is that the parton flux increases with \sqrt{s} at fixed E_T as a consequence of the fact that the distributions are tested at smaller and smaller values of x .

Experimentally, in addition to the two-jet events a considerable number of multijet events have been observed at CERN SPS $p\bar{p}$ collider. According to the above considerations, one can hope to observe, in that sample, the events generated by the multiple sub-processes. One other interesting aspect of multiparton processes is related to the information on hadronic structure that they can provide through their connections to multiparton distributions $G(x_1, x_2, \dots, x_n)$.

All these phenomenological as well as experimental considerations lead to the need of analysing properly this kind of new sub-process in the framework of perturbative QCD. The simplest process to analyse analogous to double scattering is the double Drell-Yan process⁽⁹⁾. The latter has already been studied in the simplest case of colourless and spinless quarks by C. Goebel et al. for an order of magnitude estimate and they conclude that also this process is at the limit of observability. The importance of analysing the double Drell-Yan in the QCD framework however, lies mostly on the common features it shares with the double scattering which is relevant to high P_T jet processes and whose analysis so far has been limited to qualitative estimates. A very large part of our analysis will be thus common to both processes and shows a quite new structure of multiparton processes not put properly into evidence by previous studies owing to the spin and colour structure of the interacting partons.

The spin and colour degrees of freedom introduce six newly defined structure functions $G_b^c(x_1, x_2, \dots)$ ($c=1,2$; $b=1,2,3$) for each hadron. They describe more than just the x -distributions of the parton, but contain also information about how the incoming partons are colour and spin correlated inside the hadron. These structure functions depend also on the relative transverse distance Δ_T separating, inside the hadron, the two incoming partons. It should be mentioned however that the Δ_T dependence is not a quantum mechanical effect. The transverse distance Δ_T separating the two incoming partons inside the parent hadron already appears in the definition of the double density functions in the analysis of the double collision from the point of view of classical mechanics.

The study of the double Drell-Yan mechanism is conceptual and proposes to properly formulate the problem in the context of the now well-admitted theory of QCD.

The thesis is organized as follows: in section II, devoted to the phenomenology of disconnected processes, we review successively the multi-constituent scattering as a model for elastic scattering at wide-angle, the production of baryons with large transverse momentum and account at some length for the recent phenomenological development of high P_T multi-jets, gauge boson pairs etc. produced via the double scattering mechanism. We end up the section with a brief review of the single and double Drell-yan cross sections.

Section III deals with the conceptual aspect of the multi-parton scattering, where we analyse the double Drell-Yan mechanism in the QCD framework.

II MULTIPARTON PROCESSES: PHENOMENOLOGY

A. Multi-constituent scattering as a model for elastic scattering at wide angle

A1 Introduction

There is a considerable amount of accurate data from wide-angle proton-proton elastic scattering at high energies. For s , the C.M. energy between 15 and 60 GeV^2 and $|t| > 2.5 \text{ GeV}^2$, an excellent fit to these data is given by

$$\frac{d\sigma}{dt} \sim s^{-n} f(\theta) \quad (1.A)$$

with $n \approx 9.7$, here θ is the C.M scattering angle. It is widely assumed that these simple features of the data indicate that some sort of asymptotic regime, for s and t both large, has set in and further that they are a manifestation of a constituent structure of the scattering hadrons. However the mechanism underlying these constituent scattering is not quite clear and indeed various models^(5,10,11,12) are proposed to account for the result (1.A). In most of the models, it is assumed that only one constituent of each hadron plays an active role in the scattering, in the sense that it alone is exchanged or, alternatively scatters directly on a constituent of the other hadron according to the precise version of the model (Fig. 1A)

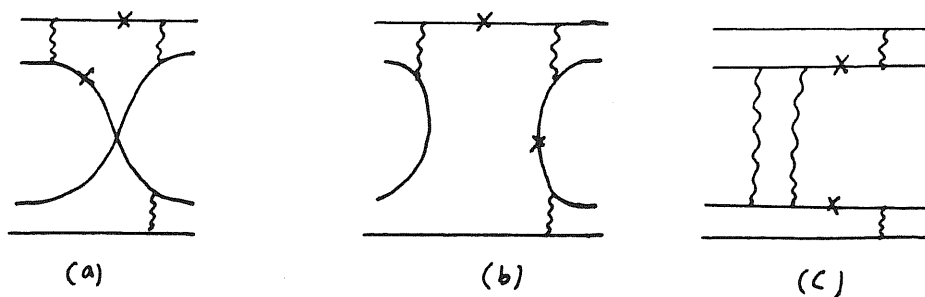


Fig. 1A: Models already proposed for $\pi\pi$ wide angle elastic scattering; The cross refers to "hard propagator".

A crucial consequence of these models is that the scattering depends on constituents that have a large component of momentum transverse to the momentum of their parent hadron. Therefore, the differential cross section that results for the scattering is small because such constituents are found comparatively rarely. Also in these models there exist "hard propagators" which subsequently reduce the resulting amplitude.

An alternative and original model has been proposed by Landshoff, in which, contrary to previous models (single scattering) it is assumed that the important contribution to the cross section comes from constituents with vanishing transverse momenta. The model is referred to as the multiparton-scattering model⁽¹⁾.

We shall review in detail here the multiparton-scattering mechanism and show to what extent it may play a role in the description of exclusive processes. The generalization of the mechanism to inclusive processes will be the subject of the following sections.

A2 Description of the multiparton scattering

a) Lowest order QCD results

Each initial-state hadron is pictured as breaking up into a number of constituents whose momenta are all more or less collinear to the momentum of their parents; each constituent of one hadron then scatters at wide angle on at least one constituent of the other hadron in such a way that after the scatterings, the momenta of the constituents are so aligned that they can readily recombine to make up the final-state hadrons (Fig. 2A). This roughly means that the scattering occurs at equal angles. In this case it is mainly this limitation of the phase space (to be opposed to the existence of hard propagators in conventional single scattering models) which reduces the elastic cross section. This limitation is however not necessary for inclusive processes where we do not expect such phase space suppression.

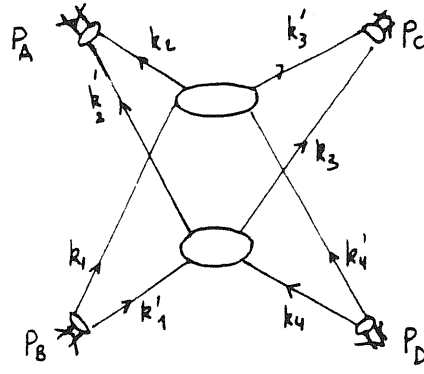


Fig. 2A: Model used for $\pi\pi$

The complexity of the interaction increases with the number of hadronic constituents. Thus it is assumed here that the pion for instance is regarded as being composed of a single quark-antiquark pair. It should be noted however that such an assumption is not needed in the description of inclusive cross sections where spectator quarks also participate. In the diagram of Fig. 2A, the four external vertices are coupling functions that restrict the momentum components of the quarks transverse to the momentum of their parent hadron, and also their off-shellness. For $\pi\pi$ scattering and to lowest order⁽¹³⁾ in perturbative QCD, there are two topologically distinct diagrams, shown in Fig. 3A

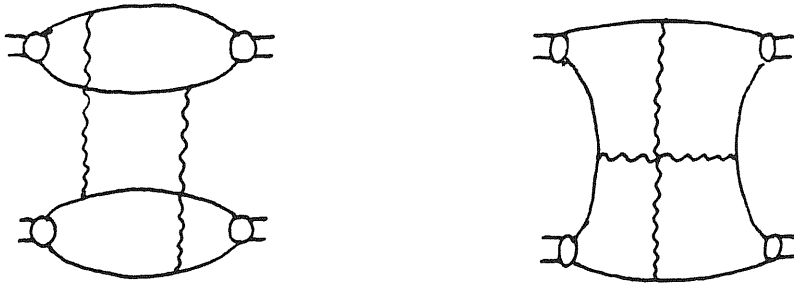


Fig. 3A: Dominant diagrams for $\pi\pi$ scattering at lowest order

Further diagrams are obtained from these by crossing. The spinor structure of the external vertex functions is taken into account, assuming a simple γ_5 coupling of the pion to the quarks, together with a form factor to provide the necessary damping, hence the coupling of the pion to the quarks is taken of the form

$$\gamma_5 g(k^2, k'^2). \quad (2.A)$$

Having specified all the elements of the amplitude (Fig. 2A), one can work out the differential cross section for the elastic scattering at wide angle. The model gives a result which has the simple structure of formula (1.A). The result comes essentially from a phase-space calculation

$$\frac{d\sigma}{dt} \sim \frac{ct^2}{s^3 t u} \sim s^{-5} f(\theta) \quad (3.A)$$

where s , t and u stand for the usual Mandelstam invariants. This result corresponds to $n=5$ for $\pi\pi$ scattering in formula (1.A) since $s \sim t \sim u$.

It is very important to notice that the multiparton scattering model we are dealing with predicts a quite different result with respect to those obeying the dimensional counting rule⁽⁵⁾ (DCR) which gives instead $n=6$ for $\pi\pi$ scattering. We recall here that the dimensional counting rule predicts that the differential cross section for the scattering $AB \rightarrow CD$ at large t has a form that depends on the total number of valence constituent quarks in the four participating hadrons

$$\frac{d\sigma}{dt} \sim s^{-\eta} f(\theta) \quad (4.A)$$

$$\text{where } \eta = \eta_A + \eta_B + \eta_C + \eta_D - 2.$$

which corresponds effectively to $n=6$ for $\pi\pi$ scattering. Therefore one would expect the process under study to dominate the ordinary ones briefly introduced in Fig.(1A). The corresponding model for nucleon-nucleon scattering where each nucleon is regarded as a bound state of three quarks is drawn in Fig. (4A).

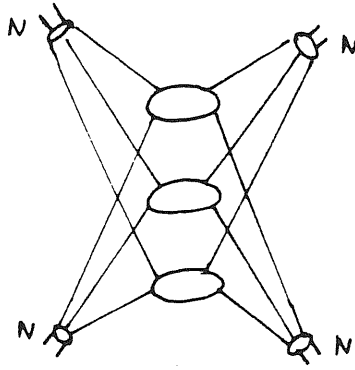


Fig. 4A: Model for N-N scattering

The differential cross section corresponding to N-N scattering has the form

$$\frac{d\sigma}{dt} \sim \frac{ct_i}{s^4 t^2 u^2} \sim s^{-8} f(\theta). \quad (5.A)$$

This corresponds to $n=8$ in formula (1.A) which has to be compared with the value $n=10$ obtained for the conventional single scattering mechanism from dimensional arguments. The associated function $f(\theta)$ has a complicated form and its detailed structure depends on the structure of the hadron wave-function. However for momentum transfers $-t \ll s$, the single exchange of spin-1 gluon makes $f(\theta)$ independent of θ , so that

$$\frac{d\sigma}{dt} \sim t^{-8} \quad (6.A)$$

with no dependence on s at fixed t . The data at FNAL and ISR energies are in agreement with this prediction, being essentially energy-independent and fitting well to the shape t^{-8} . This is however in contrast with lower energies where there is a very marked energy dependence and the value of n is close to 10 which is the value predicted by DCR.

So far the multiparton scattering at the lowest order in QCD seems to play an important role in the dynamic of exclusive processes and one is tempted to see how much higher order QCD corrections will

modify the simple result of formula (1.A). It has been suggested however by various authors^(14,15,16,17) that higher order corrections to the double scattering mechanism will result in important modifications.

b) Higher order corrections to multiparton scattering in exclusive processes

The problem now is to consider radiative corrections to the diagrams of Fig. (3A). There are two kinds of radiative corrections. They involve what we shall call from now on "non-connecting gluons" and "connecting gluons". The former correct the hard scatterings individually, like for instance, the vertex corrections; the latter connect the two separate parton-parton scattering. Examples of connecting gluons are drawn in Fig. 5A.

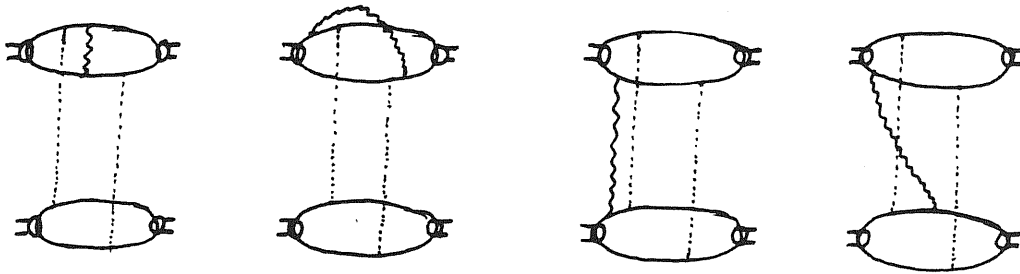


Fig. 5A: Examples of connecting gluons (wavy lines)

Connecting and non-connecting gluons are quite similar with however a very remarkable difference, that is the component k_T of the connecting gluon, transverse to all external momenta of the diagram cannot become large without the transverse momentum flowing through at least one of the pion wave-functions becoming large. This simply means that, according to the previous assumption on the behaviour of the hadron wave function, k_T is bounded. We shall see that this important feature is common to all disconnected processes.

The important contributions of both kinds of gluons come from their soft components and so the problem is to analyse the infra-red behaviour of all possible diagrams. We shall not enter into details here but only mention the main results of these computations. For more details see Reference (2) and the Appendix.

For fixed non-zero scattering angle θ , one finds that in the leading log approximation (LLA) the effect of inserting an additional gluon in the multiparton scattering is to modify the result (1.A) by the factor

$$-b \ln^2 s$$

with $b = \frac{g^2}{2\pi^2} \frac{N-1}{N} n$

(7.A)

where g is the coupling constant, $N=3$ is the number of colour and n is the number of multiple scattering i.e. $n=2$ for $\pi\pi$ and $n=3$ for pp .

Adding a second additional gluon gives instead of (7.A) the factor

$$\frac{1}{2} b^2 \ln^4 s$$
(8.A)

So it seems likely that in (LLA) order by order, the effect of adding any number of gluons is to multiply the result (1.A) by an exponential factor

$$\exp(-b \ln^2 s).$$
(9.A)

This result agrees with the conjectures of previous authors^(14,15,16,17), except that there is a larger number of important diagrams that had been suspected and in consequence b is smaller than had been supposed, by a factor 2.

We note here that the result (9.A) is obtained by the formal procedure of extracting the leading behaviour diagram by diagram, and

then summing. Because the resulting sum (9.A) goes to zero very rapidly when s is large, it could well be that lower order contributions from the individual diagrams sum to a more important result.

The computation of various diagrams leading to this exponential factor are restricted to the case where $s \sim t$ so that $\ln s \sim \ln t$. It is found that when t is large but much less than s , additional diagrams (involving the triple gluon vertex) become important. Up to two additional gluon insertions the factor that multiplies the result (1.A) again exponentiates

$$\exp(-2b_1 \ln s \ln t + b_2 \ln^2 t). \quad (10.A)$$

with

$$b_1 = \frac{g^2}{8\pi^2} N n .$$

$$b_2 = \frac{g^2}{8\pi^2} \frac{N+1}{N} n .$$

The exponential (Sudakov) form factor obviously falls faster than any power of s as $s \rightarrow \infty$ so that in the end, the multiple exclusive cross section will be asymptotically suppressed with respect to the conventional single scattering, obeying the DCR. Phenomenologically at present energies the situation is not clear: probably what one sees is a combination of the two effects. The presence of the "Sudakov double log" in multiparton scattering (exclusive processes) can be easily explained and occurs in the following way. The diagram (6Aa) has a double logarithm i.e. is proportional to $\ln^2 t$ (vertex correction), since we have both infra-red and mass singularities. One of these logarithms comes from the k_T integration of the corresponding gluon which is

$$\int_{p^2}^t \frac{dk_T^2}{k_T^2} \sim \ln\left(\frac{t}{p^2}\right). \quad p \text{ is the quark momentum (11.A)}$$

The only diagram able to cancel the double log of diagram (6Aa) is the diagram of (6Ab). However we have already said that the k_T associated with connecting gluons has a cut-off of order

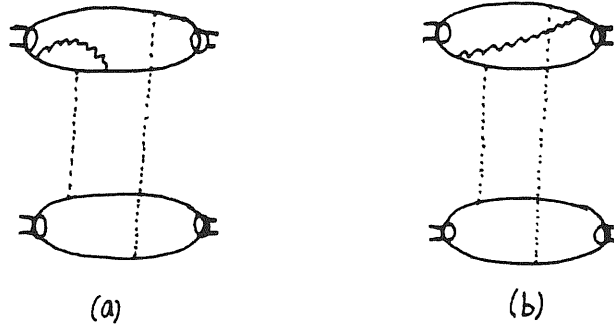


Fig. 6A: diagrams (a) and (b) do not cancel each other.

$(\frac{1}{R})$ where R is the hadronic size, therefore the corresponding integral is independent of t and no cancellation of the double log factor occurs. There seems to be no way of avoiding a Sudakov suppression of the multiparton scattering diagrams in exclusive reactions. The suppression of the multiparton scattering mechanism in the area of exclusive processes is due precisely to infra-red double log factors as we have already seen. These unwanted contributions can be cancelled however by real gluon contributions if one allows initial and/or final partons to radiate real gluons, which we have not allowed in the exclusive cross section. Therefore one may expect the multiparton scattering not to be affected by Sudakov suppression in the description of inclusive reactions e.g. hadron production at large P_T , multijet systems etc. where partons are allowed to radiate in all possible ways, more precisely over the available phase space.

In the following sections we shall describe the physics of inclusive multiparton scattering showing the progress made in this direction and point out the new features which are inherent to this mechanism.

B. Production of baryons with large transverse momenta via the multiple scattering mechanism

B1 Introduction

Experimental data on the production of hadrons at large transverse momentum P_T are generally summarized in the following simple formula⁽¹⁸⁾

$$E \frac{d\sigma}{d^3p} = P_T^{-n} f(x_T, \theta). \quad x_T = \frac{2P_T}{\sqrt{s}} \quad (1.B)$$

with θ , the centre of mass angle of the out-going proton. The effective value of n varies with X_T and at large X_T it remains nearly constant with the value $n=8$ for mesons and $n=14$ for protons. It is also found experimentally that the production of high P_T baryons is surprisingly copious.

While there are a number of theoretical models⁽¹⁹⁾ proposed to explain the production of mesons at large P_T , the corresponding production of protons has proved more difficult to understand⁽²⁰⁾. The single scattering model in the framework of QCD cannot explain formula (1.B) for protons, since it gives too slow a value for n ($n=4$) at the parton level. It has been shown by various authors^(21,22) however that scaling violations can enhance the above value, thus making the model (single scattering plus QCD) adequate for large P_T meson production. However one does not see how the model could manage to reach the rather high value $n=14$, since in the parton model description of large P_T hadrons, mesons and protons cross sections are similar in form and differ just in the definition of the fragmentation functions which are dimensionless quantities.

The authors of reference (23) proposed as an alternative the multiparton scattering model to describe the production of protons at

high P_T . They work out the corresponding cross section which has the form of formula (1.B) with the desired value $n=14$, provided the hard scattering are scale invariant (in current computations one can take QCD Born term which is scale free). We shall briefly expose the model in the next section and introduce some of the materials necessary for the forthcoming studies.

B2 Description of the model

The proposed mechanism for the production of baryons at large P_T is shown in Fig. (1Ba)

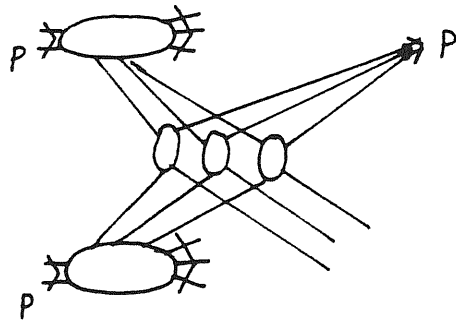


Fig. 1Ba: The triple-scattering mechanism for the production of a large P_T proton

Each proton emits three quarks of finite "mass" and with momenta closely aligned with the momentum of their parent. Each quark from one of the proton scatters on a quark from the other proton in such a way that there are three closely aligned quarks in the final state capable of recombining to produce the observed large P_T proton. The other three quarks which have undergone a wide-angle scattering into the final state do not have to recombine into a definite single baryon. Their combined invariant mass is, in general large so that they are expected to materialize as a system of hadrons, usually one baryon and a number of mesons.

The differential cross section $E \frac{d\sigma}{d^3p}$ is related to the discontinuity in the missing mass of the following forward elastic scattering Fig. (1Bb).

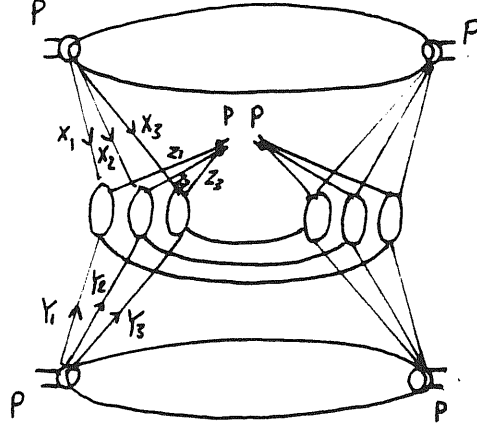


Fig. 1Bb: The Mueller diagram for the process of Fig. 1Ba

The authors of reference (23) have been able, in the spinless and colourless case, using dimensional arguments, to work out an approximate form for the cross section at sufficiently large s and P_T . They write the result as

$$E \frac{d\sigma}{d^3p} \sim \frac{1}{P_T^2 s^6} \int dx_1 dx_2 dx_3 dy_1 dy_2 dy_3 dz_1 dz_2 dz_3 G_A(x_1, x_2, x_3) G_B(y_1, y_2, y_3) D(z_1, z_2, z_3) \delta(z_1 z_2 z_3 - 1) \prod_{i=1}^3 \delta\left(\frac{x_i r_i}{x_i \cot \frac{1}{2}\theta + y_i \tan \frac{1}{2}\theta} - \frac{P_T z_i}{\sqrt{s}}\right) \prod_{i=1}^3 [T(x_i, y_i, z_i)]^2. \quad (2.B)$$

Here $G_A(x_1, x_2, x_3)$ is interpreted as the probability to find three constituents with fractional momenta x_1, x_2, x_3 simultaneously within the nucleon and similarly for $G_B(y_1, y_2, y_3)$. The function $D(z_1, z_2, z_3)$ is the square of the wave function for the nucleon being in its pure three-quark configuration (with no sea), the quarks having fractional momenta z_1, z_2 and z_3 . The amplitude $T(x_i, y_i, z_i)$ which is dimensionless corresponds to the central wide-angle scattering. The above

formula can be seen to correspond effectively to $n=14$ in formula (1.B), in fact

$$E \frac{d\sigma}{d^3p} \sim \frac{1}{P_T^2 S^6} \sim \frac{1}{P_T^{14}} \quad \text{at fixed } x_T = \frac{2P_T}{\sqrt{S}} \quad (3.B)$$

This is one of the most important predictions of the model. Now it is an experimental fact that the value of n is x_T -dependent, more precisely it increases asymptotically with x_T and reaches the value $n=14$ at very large x_T . In this regime the lowest order QCD diagram (i.e. parton model) give a good prediction ($n=14$). The increase of n with x_T is also well accounted for in the multi-scattering model but we do not discuss that here but rather refer to the literature⁽²³⁾.

Another qualitative prediction of the model is that the function $f(x_T, \theta)$ in formula (1.B) has the important property

$$f(x_T, \theta) \text{ remains finite as } x_T \rightarrow \sin \theta \text{ for any fixed } S \quad (4.B)$$

In fact, all subprocesses are forced to the edge of their phase space in the limit ($x_T \rightarrow \sin \theta$), so that the effect is that the top and bottom blobs of Fig. (1Bb) i.e. G_A and G_B , are evaluated in the limit in which the emitted partons take all the available momentum. In the analogous situation this forces the relevant amplitudes of single-hard scattering to vanish. This is not the case for multiparton scatterings since the disconnected contributions to the blobs, e.g. Fig. 2B.

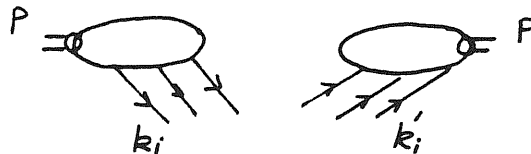


Fig. 2B: Disconnected contributions to the top blob of Fig. (1Bb).

remain non zero in this limit. That is, as $x_T \rightarrow \sin \theta$ the figure (1Bb) reduces simply to the case where the incident protons couple to just three quarks, just as in the proton-proton elastic scattering of Fig. (4A). Therefore the multiparton scattering mechanism is the only known one which does not vanish towards the edge of phase space ($x_T \rightarrow \sin \theta$) so that it must dominate at sufficiently large x_T for any fixed s .

So far, we have seen that multiparton scattering could play a central role in the description of high P_T hadron production at least at the parton level. The scaling violations introduced by collinear gluon radiations in QCD can modify the P_T dependence of the parton-parton hard scattering. Therefore a triple-quark scattering of Fig. (1Ba) (the authors of reference (23) did not specify the theory for the hard scattering) will give the experimental value i.e. $n=14$ only at the parton level (QCD Born term). It has not yet been discussed whether gluonic corrections to the proposed triple-quark scattering will modify the P_T -dependence of the cross section, as it is in the case of single scattering, or whether different gluonic contributions will arrange themselves in such a way as to preserve the formula (1.B) with the correct value $n=14$.

We have said that in order to produce a large P_T hadron, final state quarks should be closely aligned, thus allowing the recombination into the observed hadron. The resulting cross section is reduced by the restricted phase space. In the following sections we shall be interested in the inclusive jet production, where such limitation of phase space is completely absent, thus enhancing the measured cross section.

C. Multiparton scattering and large P_T jet production in hadronic collisions at collider and tevatron energies

C1. Introduction

At observed transverse energy E_T larger than 40-60 GeV, jet events start to dominate in the high P_T hadronic production as indicated by the CERN $p\bar{p}$ collider experiments⁽²⁴⁾. Apart from the copious and familiar two-jet configurations predicted by the leading QCD parton model, a great amount of three-jet and four-jet events have been also observed⁽²⁵⁾. These events might be produced via the leading QCD mechanism similarly to the e^+e^- case where also multi-jet events show up⁽²⁶⁾. In hadron-hadron collisions, the composite structure of the beam and the target permits a rather large number of quark and gluon processes to occur⁽²⁷⁾. This complex hadron structure also allows the partons of the projectile and of the target to undergo a nuclear-like multiple collision with large transverse momenta described in the previous sections. This type of interaction will contribute a large amount to the high P_T multi-jet cross sections in some kinematical regions ($E_T \ll S$) as will be shown in the forthcoming subsections^(7,8,28). In this section we shall concentrate on this last aspect and discuss at some length the role of the multi-parton-scattering mechanism in the production of three and four jets at large P_T . Two processes will be considered which have the same order in the strong coupling constant α_s . These are the disconnected double scattering and the rescattering process represented in Fig. (1Ca) and Fig.(2C).

C2. General considerations on power behaviour of the cross-sections

Let us start by recalling that one can naturally classify the various possible processes producing n -large P_T jets on a dimensional basis. The leading hard amplitude in the QCD parton model is character-

ized by two incoming parton lines and any number of outgoing ones (n), with the condition that all the kinematical invariants are large and of order of the reaction C.M energy squared S ($S \rightarrow \infty$, $t_i \sim S$ $i = 1, \dots, n$). To these amplitudes correspond an order \sqrt{s} and also a power of $(\frac{1}{S})$ (all the kinematical invariants t_i being of the same order, one chooses S for convenience). This power of $\frac{1}{S}$ depends on the number of the external lines and can be obtained from the familiar DCR based on dimensional arguments (neglecting log factors).

If one increases the number of incoming lines, giving rise to a multiple disconnected subprocess, the situation is quite different in the sense that some of the kinematical invariants in the hard process are no longer constrained to have large value of the order of S . For instance the invariant mass of two incoming partons belonging to the same hadron is not allowed to grow with S but is rather limited by the hadronic size of order R , where R is a typical hadron dimension ($R \sim 1\text{Fm}$). Therefore increasing the number of incoming parton-lines which subsequently undergo multiple disconnected hard scatterings introduces new dimensions other than S into the cross section. The corresponding contributions to multi-jet production will be depressed with respect to the leading ones by powers of $\frac{1}{R^2 S}$ if one keeps the constraints that $t_i \sim S$ and therefore the leading terms will still safely dominate the n -jet production cross sections. There are however some kinematical regions where some of the t_i although much larger so that we are still in the QCD perturbative regime are much smaller than S , the terms of order $\frac{1}{R^2 t_i}$, might however in that case not be so negligible. An estimate of the suppression factor for a moderate value of $t_i \sim 1000 \text{ GeV}^2$ and $R \sim 1\text{Fm}$ gives a value $\sim 10^{-4}$. This seems to be quite big a suppression. The point is that independently of dimensionalities, the steepness of the cross-section in the P_T of the jets has a crucial role. In fact due to the steepness of the parton cross sections, it may become more economical at fixed E_T to have several parton scatterings,

each at relatively low P_T , rather than a single one with a large P_T and this could allow for an appreciable comeback on the suppression factor.

Another intuitive way to understand the $\frac{1}{P_T^2 S}$ suppression factor of multiple processes is to follow the arguments developed by D. Politzer⁽³⁾ and look at the form of the disconnected double scattering cross section.

Assuming the validity of the parton model at high S for such processes one obtains

$$\sigma_D \sim \frac{1}{S} \int dx_1 dx_2 dy_1 dy_2 \tilde{G}_A(x_1, x_2, M^2) \tilde{G}_B(y_1, y_2, M^2) \delta^4(0) |T_1|^2 |T_2|^2. \quad (1.C)$$

where T_1 and T_2 are the hard two into two parton amplitudes and are dimensionless according to DCR. The $\delta^4(0)$ is the singularity associated with Collinear quarks and which characterizes the disconnection of the process.

The formula (1.C) has extra dimensions with respect to the leading QCD term (single scattering), they are carried by the quantity

$$\tilde{G}_A(x_1, x_2, M^2) \tilde{G}_B(y_1, y_2, M^2) \delta^4(0). \quad (2.C)$$

The mass M^2 is an arbitrary momentum scale introduced to divide soft from hard effects. The point now is to extract the dimensions of the quantity (2.C). The singularity $\delta^4(0)$ comes from the plane wave convention and is similar to that appearing in the proper definition of a cross section. It only appears because we treat the incoming partons as plane waves, which then scatter everywhere for all times. Therefore it actually represents the space time volume of the second collision relative to the first one, and is easily estimated in the C.M frame. The second pair must collide within the same hadron-hadron spatial volume sometimes while hadrons overlap. The hadron's transverse

dimensions are uncontracted in the C.M frame, but their longitudinal diameters are of order $\frac{1}{E}$, where E is their energy. The time in the C.M frame for which these two relativistic pancakes overlap is also order $\frac{1}{E}$. Hence one makes the identification

$$\delta^4(0) \rightarrow \frac{\pi R^2}{E \times E} \sim \frac{\pi R^2}{S} \quad (3.C)$$

Now the double-constituent distribution functions \tilde{G}_A and \tilde{G}_B are dimensionful and may be written as

$$\begin{aligned} \tilde{G}_A(x_1, x_2, M^2) &= M^2 G_A(x_1, x_2) \\ \tilde{G}_B(y_1, y_2, M^2) &= M^2 G_B(y_1, y_2) \end{aligned} \quad (4.C)$$

If one chooses $\frac{1}{M^2}$ to be a hadronic cross sectional area i.e. $M^2 = \frac{1}{\pi R^2}$, the quantity (2.C) will be of the form

$$\tilde{G}_A(x_1, x_2, M^2) \tilde{G}_B(y_1, y_2, M^2) \delta^4(0) \sim \frac{1}{R^2 S} G_A(x_1, x_2) G_B(y_1, y_2). \quad (5.C)$$

Therefore the suppression factor with respect to single scattering is $\frac{1}{R^2 S}$.

C3. The large- P_T multi-jet cross section formulae

The purpose of the following analysis is to report some estimates of the double-parton scattering contribution to the large- P_T multi-jet cross section in high energy $p\bar{p}$ collision. The form of the double cross section has been worked out by the authors of references (7,8,23). This form will serve as the starting point of all the forthcoming phenomenological applications. The theoretical study of the double scattering cross-section is however incomplete in the sense that

it does not account for the parton colour and spin degrees of freedom. In the last section we shall analyse the double Drell-Yan cross section and show that the colour and the spin are a nontrivial complication in the description of multi-parton processes. To have an idea about the form of the double scattering cross section we consider the simplest case of the 4-jet system shown in Fig. (1Ca).

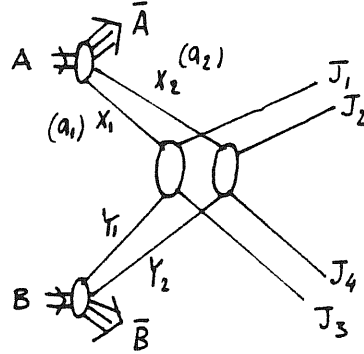


Fig. 1Ca: The 4-jet process under consideration

The cross section for the above process is given by

$$(2(2\pi)^3)^2 E_{J_1} E_{J_2} \frac{d\sigma}{d^3J_1 d^3J_2} = \frac{1}{2S} \text{Disc}_{(S)} \mathcal{M}(A, B, J_1, J_2). \quad (6.C)$$

Where $\mathcal{M}(A, B, J_1, J_2)$ is the forward elastic amplitude (Mueller) corresponding to the diagram of Fig. (1Ca). We sketch in Fig.(1Cb) its corresponding diagram

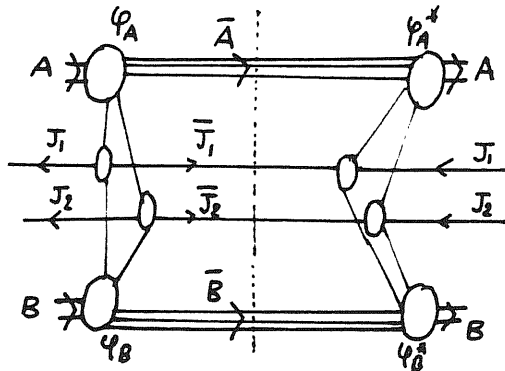


Fig. 1Cb: Feynman diagram for the amplitude $\mathcal{M}(A, B, J_1, J_2)$.

To compute the forward amplitude $M(A, B, J_1, J_2)$ one has to perform complicated integrations where all the momenta are involved. At the first sight, due to the complexity of the integrations, one would expect interferences to be important. Writing the jet cross section only in terms of kinematical variables which grow with \sqrt{s} and neglecting all those of order $\frac{1}{\sqrt{s}}$, the various integrations in eq. (6.C) get disentangled. Keeping only leading terms in $\frac{1}{\sqrt{s}}$ is not enough to get a probabilistic interpretation of the jet cross section. In order to achieve that, one introduces Fourier transforms with respect to the transverse variables

$$\tilde{\psi}\left(\frac{q_1+q_2}{2}, q_1-q_2, \lambda\right) = \frac{1}{(2\pi)^2} \int e^{i(\alpha_1 q_{1T} + \alpha_2 q_{2T})} \psi(q_{1T}, q_{2T}, \lambda) d^2 q_{1T} d^2 q_{2T}. \quad (7.C)$$

$\psi(q_{1T}, q_{2T}, \lambda)$ describes the hadronic initial state, α_1, α_2 indicate the transverse coordinate and λ refers to the longitudinal degrees of freedom. Therefore one gets a probabilistic interpretation of the cross section in terms of the "impact parameter" $\Delta_T = q_1 - q_2$ (relative transverse distance separating the two incoming partons inside the hadron) and not in terms of their relative transverse momentum. The structure functions which describe the initial hadrons get dependent on x_1, x_2 and Δ_T . It is shown⁽⁷⁾ that the structure function $G_A(x_1, x_2, \Delta_T)$ is related to the vertex function $\varphi_A(q_1, q_2, \bar{A})$ by the relation (and similarly for $G_B(x_1, x_2, \Delta_T)$)

$$G_A(x_1, x_2, \Delta_T) = \frac{5 x_1 x_2}{2(1-x_1-x_2)} \frac{1}{(2\pi)^6} \int |\tilde{\psi}_A|^2 d^2 \Delta_T \quad (8.C)$$

where $\tilde{\psi}_A$ is the Fourier transform, see eq. (7.C) of ψ_A which in turn is related to φ_A through

$$\psi_A(q_{1T}, q_{2T}, (a_1)_+, (a_2)_+, \bar{A}) \equiv \int \frac{\varphi_A(q_1, q_2, \bar{A})}{D(a_1) D(a_2)} \frac{d\sigma}{2\pi} ; \quad \Delta_T = \frac{q_1 - q_2}{2} \quad (9.C)$$

$D(a_1), D(a_2)$ are the quark propagators.

The authors of reference (7) arrive at the following expression for the cross section which has a very simple form (for details about its derivation see their reference).

$$E_1 E_2 \frac{d\sigma}{d^3y_1 d^3y_2} = \sum_{[a,b]} \int G_A(x_1, x_2, \Delta_T) G_B(k_1, k_2, \Delta_T) \frac{\hat{s}_1}{\pi} \frac{d\hat{r}}{d\hat{t}_1} \frac{\hat{s}_2}{\pi} \frac{d\hat{\sigma}}{d\hat{t}_2} \delta(\hat{s}_1 + \hat{t}_1 + \hat{u}_1) \delta(\hat{s}_2 + \hat{t}_2 + \hat{u}_2) dx_1 dx_2 dk_1 dk_2 d\Delta_T. \quad (10.C)$$

where the Mandelstam invariations \hat{s} , \hat{t} , \hat{u} refer to the hard subprocess and the sum is over all independent subprocesses. Equation (10.C) has some analogies to the expression one obtains for the single large P_T jet cross section. The dependence on the target and the projectile is represented in this equation by the multiconstituent distributions $G_A(x_1, x_2, \Delta_T)$ and $G_B(y_1, y_2, \Delta_T)$ generalizing the familiar structure functions. We note here again the extra dependence of these functions on the variable Δ_T which is the relative transverse distance separating the incoming partons inside the parent hadron. The dependence on Δ_T can be easily understood by observing that the two partons of A and the two partons of B must be at the same relative transverse distance, in the limit where the two hard interaction regions vanish.

The leading behaviour of the cross section (10.C) with S can be easily obtained using the scaling behaviour of $\frac{d\hat{\sigma}}{d\hat{t}} \sim \frac{1}{\hat{s}^2}$ (up to log factors) and the fact that the dimension of $G_{A,B}$ is $\frac{1}{R^2}$ where R is the hadronic size, therefore we get for finite X_T

$$E_1 E_2 \frac{d\sigma}{d^3y_1 d^3y_2} \sim \frac{1}{R^2 S^4} \quad X_T = \frac{2E_T}{\sqrt{S}}. \quad (11.C)$$

As expected, for X_T large i.e. all the kinematical invariants t , u , etc. are of the same order as S, the process under study is suppressed by $\frac{1}{R^2 S}$ with respect to the dimensional behaviour $\frac{1}{S^3}$, so that,

for energies at which this last is reached, it would represent a very small contribution.

In order for the double-scattering to give a non-negligible contribution with respect to the leading cross-section, one may look to the small X_T region.

To work out the cross section at small X_T we cast it in terms of the jets transverse momenta which grow with S and rapidities.

Noticing that the external jet variables $(J_1+J_3)_T$ and $(J_2+J_4)_T$ are small and of order $\frac{1}{R}$, we integrate over these and take as independent variables $J_{1T}, J_{2T}, y_i (i=1, \dots, 4)$. We therefore define the quantity

$$\frac{d\sigma}{d^2J_{1T} d^2J_{2T} dy_1 dy_2 dy_3 dy_4} = \int \frac{E_1 E_2 E_3 E_4}{d^3J_1 d^3J_2 d^3J_3 d^3J_4} d^2(J_{1T}+J_{3T}) d^2(J_{2T}+J_{4T}). \quad (12.C)$$

starting from equation (10.C) one can get the expression corresponding to the cross section (12.C) which has the following form

$$\frac{d\sigma}{d^2J_{1T} d^2J_{2T} dy_1 dy_2 dy_3 dy_4} = \sum_{q/g} \int d\Delta_T G_A(x_1, x_2, \Delta_T) G_B(y_1, y_2, \Delta_T) \frac{\hat{s}_1}{\pi} \frac{d\hat{\sigma}_1}{d\hat{t}_1} \frac{\hat{s}_2}{\pi} \frac{d\hat{\sigma}_2}{d\hat{t}_2} \frac{1}{S^2}. \quad (13.C)$$

The cross section (13.C) has the physical property that at $E_T \ll S$ where E_T is the total transverse energy, it is suppressed by a factor $\frac{1}{R^2 E_T^2}$ and not $\frac{1}{R^2 S}$ (as it might appear at first sight) with respect to the leading perturbative QCD cross section for producing four jets. The kinematical region of interest ($E_T \ll S$) corresponds in fact to configurations with small incoming fractional momenta x_i, y_i ($i=1,2$). In these configurations one may expect the parton distributions to have the following behaviour.

$$G_A(x_1, x_2, \Delta_T) \sim \frac{g_A(x_1, x_2)}{R^2 x_1 x_2} \quad \text{and} \quad G_B(y_1, y_2, \Delta_T) \sim \frac{g_B(y_1, y_2)}{R^2 y_1 y_2}. \quad (14.C)$$

with g_A, g_B finite as $X_1, X_2, Y_1, Y_2 \rightarrow 0$. Equation (13.C) would then behave as

$$\frac{d\sigma}{d^2J_T d^2J_{2T} dy_1 dy_2 dy_3 dy_4} \sim \sum_{q/q} \frac{g_A(X_1, X_2) g_B(Y_1, Y_2)}{R^2 \hat{s}_1 \hat{s}_2} \frac{\hat{s}_1}{\pi} \frac{d\hat{\sigma}}{d\hat{t}_1} \frac{\hat{s}_2}{\pi} \frac{d\hat{\sigma}}{d\hat{t}_2}. \quad (15.C)$$

The right-hand side of Eq. (15.C) depends only on the kinematical invariants of the subprocess that is $\hat{s}_i, \hat{t}_i, \hat{u}_i$ ($i=1,2$) and not on the C.M energy \sqrt{S} , since the functions $g_A(X_1, X_2)$ and $g_B(Y_1, Y_2)$ are finite at very small X_i, Y_i and therefore the four-jet cross section of Eq. (15.C) depends on E_T and not on S .

Since the depression factor is $\frac{1}{R^2 E_T^2}$ and not $\frac{1}{R^2 S}$, which would be exceedingly small, the effect might be observable even at large C.M energy, provided E_T is (although large) limited compared to \sqrt{S} . Also the cross section can be expected to grow with increasing \sqrt{S} at fixed E_T , because smaller and smaller values of fractional momenta in the parton distributions are tested in this case; More information on these points as well as the derivation of formula (13.C) can be found in reference (7).

The other interesting process (the rescattering process) depicted in Fig. 2C which may play a role in the description of the 3-jet cross-sections have been proposed by the authors of reference (7).

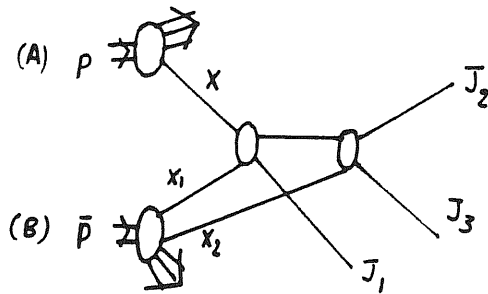


Fig. 2C: The parton rescattering process under consideration

The process is such that one parton (e.g. of the projectile) first undergoes a hard scattering, and after propagating for a long distance (of the order of the hadronic dimension R) with a low virtuality has a second hard interaction with another parton within the target. Thus the structure of the $(3 \rightarrow 3)$ amplitude in Fig. 2C would be that of two $(2 \rightarrow 2)$ amplitudes connected by an almost on-shell propagator. The cross-section corresponding to the rescattering process has the simple form

$$\frac{d\sigma}{d^2J_{1T} d^2J_{2T} dy_1 dy_2 dy_3} = \sum_{q/g} G_A(x) G_B(x_1, x_2, \Delta=0) \frac{\hat{s}_1}{\pi} \frac{d\hat{\sigma}}{d\hat{t}_1} \frac{\hat{s}_2}{\pi} \frac{d\hat{\sigma}}{d\hat{t}_2} \frac{1}{s^2 x_1} \quad (16.C)$$

As for the formula (13.C), the suppression factor with respect to the leading QCD cross section for producing three-jets will be $\frac{1}{R^2 E_T^2}$ at a given E_T .

The three and four jet processes have the same number of hard interactions. They are both of order α_s^4 , therefore they are expected to have comparable rates.

We have used the small x behaviour of the double structure functions given by formula (14.C) in the derivation of the cross section formulae (15.C) and (16.C). Here we want to make a few remarks on that behaviour.

The kinematical region we are interested in is that where $E_T \ll S$, this corresponds to small x . In this region one would expect the gluons to play an important role. If one can neglect the self-gluon coupling, one can guess rather naturally, in analogy to electrodynamics, that independent gluon emission should occur according to a Poisson-like probability distribution. For n -emitted gluons with fractional momenta x_1, x_2, \dots, x_n ⁽²⁹⁾, the distribution is of the form

$$P_n(x_1, x_2, \dots, x_n) = \frac{1}{n!} P(x_1) P(x_2) \dots P(x_n) e^{-\int_{x_{min}} P(x) dx} \quad (17.C)$$

The function $P(x)$ which characterizes the one gluon emission with fractional momentum x is the inclusive distribution for the emission of one gluon; this can be seen as follows

The single inclusive distribution

$$\begin{aligned}
&\equiv P(x) e^{-I} + \frac{1}{2} P(x) e^{-I} \int_{x_{\min}}^1 P(x_1) dx_1 + \frac{1}{2} P(x) e^{-I} \int_{x_{\min}}^1 P(x_2) dx_2 + \dots \\
&= P(x) e^{-I} (1 + I + \frac{1}{2} I^2 + \dots) = P(x)
\end{aligned}
\tag{18.C}$$

where

$$I = \int_{x_{\min}}^1 P(x) dx.$$

At small x , $P(x)$ has the diverging behaviour, therefore to make the integral in Eq. (17.C) well defined one has to introduce a cut-off x_{\min} . The exponential factor is introduced in such a way as to have

$$\sum_{n=1}^{\infty} \int P_n(x_1, x_2, \dots, x_n) dx_1 dx_2 \dots dx_n = 1. \tag{19.C}$$

The quantity of interest is rather the inclusive double distribution function $G(x_1, x_2)$. To construct it one has to sum all gluon configurations with two and more than two gluons, thus we have

$$\begin{aligned}
G(x_1, x_2) &= \frac{1}{2} P(x_1) P(x_2) e^{-I} + \frac{3}{3!} P(x_1) P(x_2) e^{-I} \int P(x_3) dx_3 + \frac{6}{4!} P(x_1) P(x_2) e^{-I} \left[\int P(x_3) dx_3 \right] \left[\int P(x_4) dx_4 \right] + \dots \\
&= \frac{1}{2} P(x_1) P(x_2) e^{-I} (1 + I + \frac{1}{2} I^2 + \dots) = \frac{1}{2} P(x_1) P(x_2).
\end{aligned}
\tag{20.C}$$

Therefore in this simple scheme, the inclusive double distribution function factorizes into two independent inclusive single distribution $P(x)$ defined above

$$G(x_1, x_2) = \frac{1}{2} P(x_1) P(x_2). \tag{21.C}$$

This form generalizes easily to the multiple inclusive distribution function $G(x_1, x_2, \dots, x_n)$ i.e.

$$G(x_1, x_2, \dots, x_n) = \frac{1}{n!} P(x_1) P(x_2) \dots P(x_n). \tag{22.C}$$

We note that in the limit $x_{\min} \rightarrow 0$ the configuration with a finite number of gluons gives a vanishing contribution to average quantities due to the presence of the exponential factor in Eq. (17.C). In order to get an average quantity different from zero one has to sum up all configurations with an arbitrary number of gluons. For example the average frac-

tional momentum carried by the emitted gluons is given by

$$\langle X \rangle = \sum_{n=1}^{\infty} \int_{x_{\min}}^{x_1+x_2+\dots+x_n} P_n(x_1, x_2, \dots, x_n) dx_1 dx_2 \dots dx_n = \int_0^1 x P(x) dx. \quad (23.C)$$

The picture outlined above, namely the factorization of the n-gluon distribution is valid only if one neglects gluon correlations of any kind (kinematics, colour, etc.). It has been however emphasized by the authors of reference (29) that self-gluon interactions spoil this simple scheme in the infra-red region.

Another important point connected with the small x region is that the parton densities increase rapidly with vanishing x and this behaviour cannot go on without violating the unitarity bound. L.V. Gribov et al.⁽³⁰⁾ have shown that at very small x such that

$$\ln \frac{1}{x} \sim \alpha_s^{-2}(Q^2). \quad (24.C)$$

semi-hard cross sections reach values comparable to the geometrical dimensions of hadrons, and what prevents the unitarity violation is the parton-parton interactions (screenings) which stop the increase of the cross sections near their unitarity limit. We sketch very briefly here how the result (24.C) comes out in the case of deep inelastic scattering and in the double log approximation (DLA). DLA means that one considers only diagrams containing the term (x being small, $\ln \frac{1}{x}$ is large)

$$(\alpha_s \ln(Q^2) \ln(\frac{1}{x}))^n. \quad (25.C)$$

It turns out that these diagrams are all ladders and where only vector particles (gluons) propagate in the t-channel of the diagram. Summing all these ladders one arrives at the following form for the structure function $G(X, Q^2)$ i.e.

$$G(x, Q^2) \sim e^{\sqrt{2} \zeta y}. \quad (26.C)$$

Here

$$y \sim \ln \frac{1}{x}$$

and

$$\zeta \sim \ln \ln Q^2$$

One can notice that the DLA result (26.C) increases rapidly at small x and in the region of validity of DLA exceeds the Froissant limit⁽³¹⁾ according to which the total cross section σ^{γ^*} must not be larger than the squared radius of interaction R , i.e.

$$\sigma^{\gamma^*} \sim \frac{\alpha_{em}}{Q^2} G(x, Q^2) < 2\pi R^2. \quad (27.C)$$

This can be rewritten as

$$\alpha_s(Q^2) \frac{Q_0^2}{Q^2} G(x, Q^2) < 1. \quad (28.C)$$

where $R^2 \sim \frac{1}{Q_0^2}$. Q_0 is the target mass and we have replaced α_{em} by α_s in the case we use a gluon as a partonometer rather than a photon.

The DLA structure function, given by Eq. (26.C) satisfies Eq. (28.C) only at $\ln \frac{1}{x} < \bar{\alpha}_s^{-2}(Q^2)$ as we have said.

C4 Numerical estimates

In the region of interest i.e. small $x_T = \frac{2E_T}{\sqrt{s}}$, the typical parton fractional momenta involved are rather small. Also in that region the most important contribution comes from $gg \rightarrow gg$ and $qg \rightarrow qg$, therefore we limit ourselves to take into account these processes only. A factorized form for the double structure function $G(x_1, x_2)$ will be assumed as has been discussed at the end of the previous section, thus we write

$$G(x_1, x_2, \vec{\Delta}_T) = G(x_1) G(x_2) (1-x_1-x_2) P(\vec{\Delta}_T) \theta(1-x_1-x_2). \quad (29.C)$$

This form Eq. (29.C) constitutes however an excellent approximation to the generalized Kuti-Weisskopf model⁽³⁹⁾. In Eq. (29.C) the factor $(1-x_1-x_2)$ takes into account the kinematical correlations among the

partons. Any power of the above factor however is permissible but this is irrelevant here since in the region we are interested in, all x are small.

The authors of reference (7) work out numerically the cross sections Eq. (13.C) and Eq. (16.C) assuming a Gaussian form for $\Gamma(\frac{1}{T})$ i.e.

$$\Gamma(\vec{\Delta}_T) = \frac{1}{\pi R^2} e^{-\Delta_T^2/R^2} \quad (30.C)$$

and taking for R the value $R \sim 1 f_m$. They also take into account scaling violations. The scale Q^2 in the single parton momentum distributions is chosen to be $Q^2 = \frac{2\hat{s}\hat{t}\hat{u}}{\hat{s}^2 + \hat{t}^2 + \hat{u}^2}$. The differential cross section for producing three and four large P_T jets at zero rapidities by the mechanism discussed above are represented in Fig. 3C and Fig. 4C in the case of the Sps collider ($\sqrt{s} = 540$ GeV) and of the Tevatron ($\sqrt{s} = 2000$ GeV), for various values of the jet total transverse energy E_T . In Fig. 3Ca and Fig. 4Ca, the results are given in the case where every jet has a transverse energy larger than 10 GeV, while Fig. 3Cb and Fig. 4Cb represent the case where the transverse energy of one of the jets starts at 5 GeV. For comparison the analogous two-jet cross section is also reported.

According to these estimates one notices that the multiple-jet cross sections are only two or three orders of magnitude smaller than the two jet cross section taken at the same value of E_T . This estimate is quite different from that given by dimensional arguments which has the value $\frac{\alpha_s^2}{R^2 E_T^2} \sim 10^{-6}$. The point is that (as we have said in the introduction to this section) at a given E_T it becomes more economical to have several parton scatterings, each at relatively low P_T , rather than a single one at very high P_T due to the steepness of the parton cross sections.

An important feature which characterizes all cross-sections is that they all rise as one goes from the SPS C.M energy to the Tevatron. The increase of the three and four jet cross-section (disconnected) is however larger than those of the leading perturbative QCD and correspondingly the relative number of events is also expected to increase. We sketch in the following table the integrated cross sections. The integrations are done from a transverse energy of 40 GeV upwards and a typical rapidity interval of two units for each jet.

CERN COLLIDER Energy $\sqrt{s} = 540 \text{ GeV}$			Tevatron Energy $\sqrt{s} = 2000 \text{ GeV}$		
	Case a	Case b		Case a	Case b
$\frac{\sigma^{(3)}}{\sigma^{(2)}}$	$\simeq 0.005$	$\simeq 0.027$	$\frac{\sigma^{(3)}}{\sigma^{(2)}}$	$\simeq 0.008$	$\simeq 0.034$
$\frac{\sigma^{(4)}}{\sigma^{(3)}}$	$\simeq 0.008$	$\simeq 0.060$	$\frac{\sigma^{(4)}}{\sigma^{(3)}}$	$\simeq 0.036$	$\simeq 0.230$

We notice in this table that the mechanism considered here represents an appreciable correction to the leading perturbative QCD processes for producing three and four jets. For these latter ones the ratios above should be respectively $\alpha_s \simeq 0.2$ and $\alpha_s^2 \simeq 0.04$.

Another numerical calculation has been done, see reference (8), in which the author estimates the cross section for the production of 4-jets via the double scattering mechanism; one of these results is shown in Fig. 5C.

The above numerical estimates, although qualitative because based on unknown structure functions and forgetting the colour and spin degrees of freedom give some hope that the above mechanism will show up with a considerable number of events, in the near future at collider $p\bar{p}$ experiments. Particularly interesting is the rather unique signature of the four-jet events, which should manifest themselves

with the transverse momentum balanced pairwise. Such an event might have been already observed by the UA1 experiment⁽⁶⁾, see Fig. 6C. Another important signature of the four-jet events is that their cross sections are independent of the angle $\theta_{J_1 J_2}$ between the two observed jets. On the contrary, the leading source of 4-jet events i.e. hard gluon radiation, sharply depends on it. Thus the two effects can in principle be distinguished.

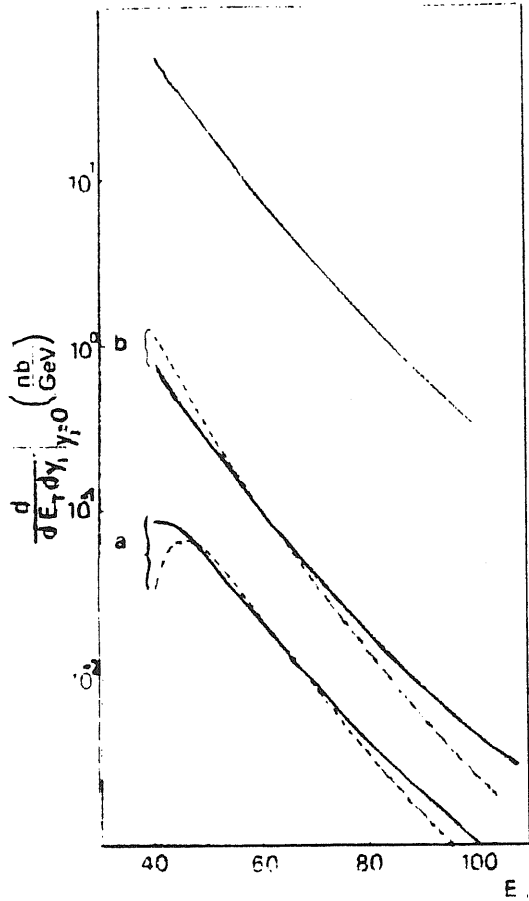


Fig. 3C

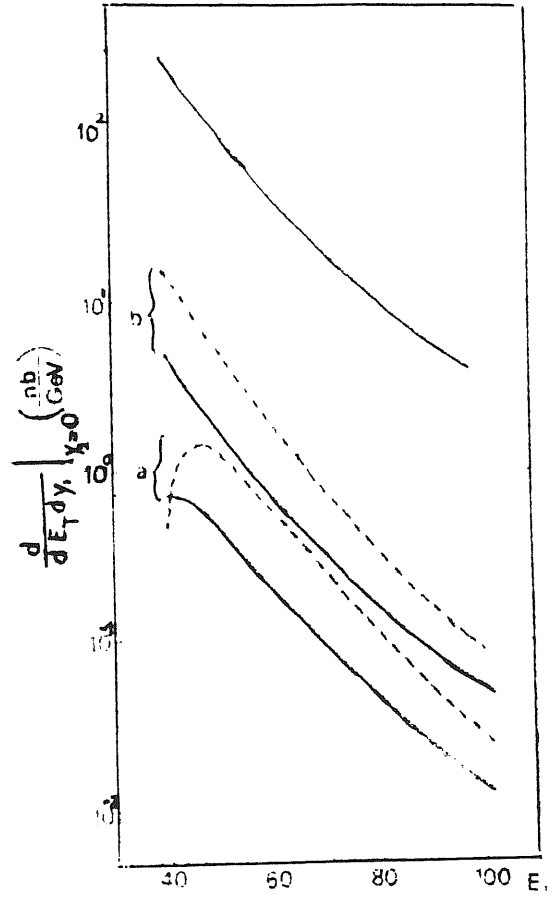


Fig. 4C

Fig. 3Ca: Three (continuous) and four (dashed) jet differential cross sections at $y_i=0$ as a function of E_T . All jets have transverse energy larger than 10 GeV; $\sqrt{S}=540$ GeV, the upper curve is the two jet cross section.

Fig. 3Cb: Same as 3Ca, but the threshold for the transverse energy of one of the jets starts at 5 GeV; $\sqrt{S}=540$ GeV.

Fig. 4Ca: Same as Fig. 3Ca, but $\sqrt{S}=2000$ GeV.

Fig. 4Cb: Same as Fig. 3Cb, but $\sqrt{S}=2000$ GeV.

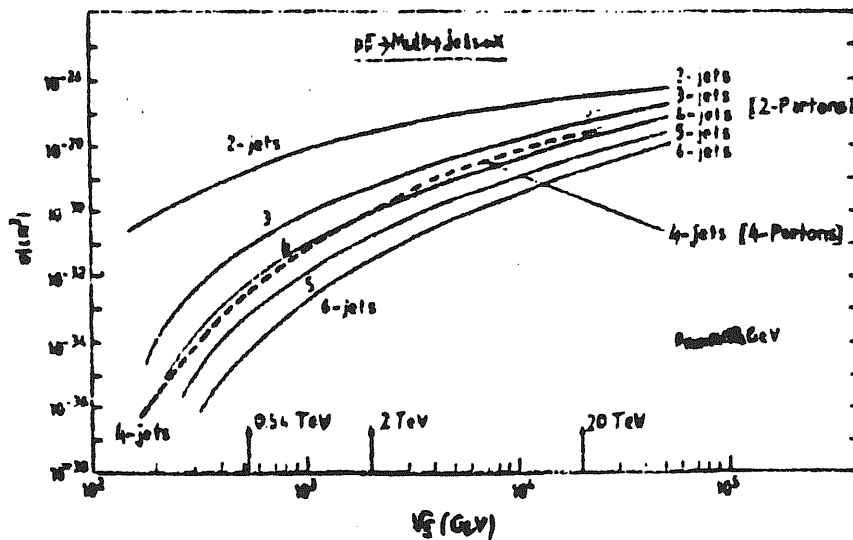
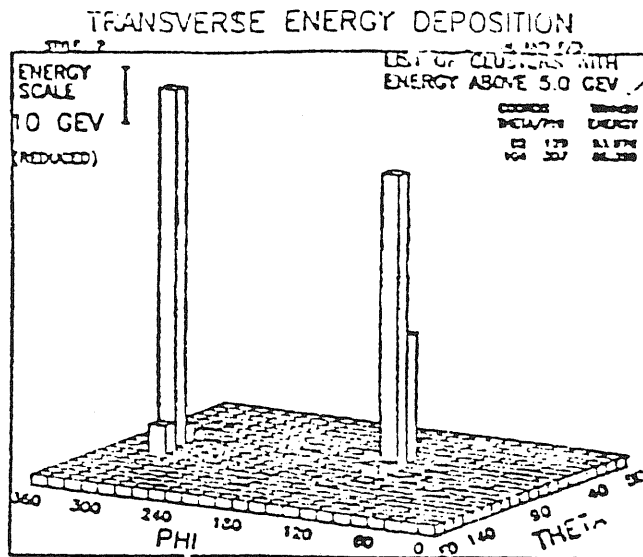
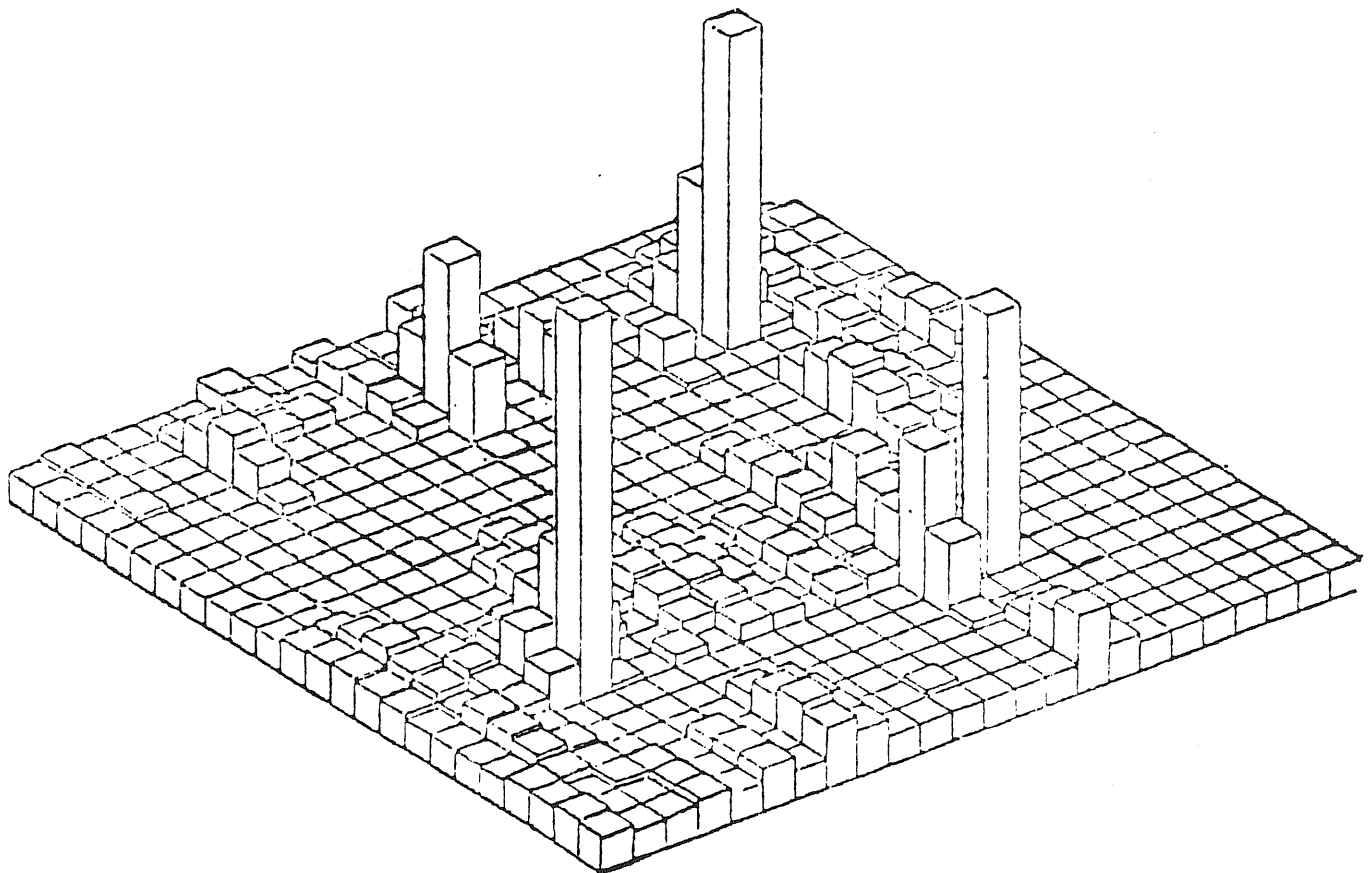


Fig. 5C

Fig. 5C: The integrated cross section for 2-, ..., 6-jet production (solid line). The transverse momentum of all jets is limited to $q_T^{\text{cut}} = 15$ GeV. In the same figure is presented the influence of the process cut q_T^{cut} (dashed line).



(a)



(b)

Fig. 6C: a) - The angular distribution of the transverse energy in the central region for a two-jet system as observed by UA1 and UA2.
 b) - The same for the four-jet systems (double hard parton scattering) observed by the UA1 experiment.

D. Production of gauge boson pairs at collider and Tevatron energies

The recent experimental observation at the CERN $p\bar{p}$ collider of the weak intermediate vector bosons W and Z has opened the possibility for their detailed study. The production of gauge boson pairs W^+W^- , W^-Z^0 , $W^- \gamma$ at pp and $p\bar{p}$ collider has been analysed by several authors⁽³³⁾.

In this section we briefly report on the work done by the author of reference (8). The aim of his study is to analyse to the lowest order (weak and electromagnetic) the production of any pair of gauge bosons initiated by 2 partons (similar to Fig. 1Da-c) together with the background originating from the 4-partons processes (Fig. 1Dd-e). The identification of a W or Z, together with another gauge boson, via a pair of hadron jets is likely to become possible, thus the quark/gluon jets of Fig. 1D-e have an imposed cut-off of $M_{jj} \gg 70$ GeV.

The set of investigated 2-parton processes is

$$q\bar{q} \rightarrow Z^0 Z^0, W^+ W^-, W^- Z^0 \quad (1.D)$$

$$q\bar{q} \rightarrow Z^0 \gamma, W^\pm, \gamma^* \gamma \quad (2.D)$$

The parton cross sections of the above subprocesses are given in Ref. (33) and (34).

Similarly, the list of analysed background 4-parton processes reads

$$(q\bar{q})_1 + (q\bar{q})_2 \rightarrow Z^0 Z^0, W^- W^-, W^+ W^-, W^- Z^0 \quad (3.D)$$

$$(q\bar{q})_1 + (q\bar{q})_2 \rightarrow Z^0 + j\bar{j}, W^+ + j\bar{j}, j^+ + j\bar{j} \quad (4.D)$$

$$(q\bar{q})_1 + (q\bar{q})_2 \rightarrow Z^0 + j_1 j_2, W^+ + j_1 j_2, j^+ + j_1 j_2 \quad (5.D)$$

where j stands for a quark/gluon jet and the rate for j^+ always involve N^+N^- (or e^+e^-) production.

In Fig. 2Da the integrated cross section of the 2-parton processes (1D) and (2D) is presented, in which the lower transverse momentum cut-off of the "direct" photon was set at $P_T = 5, 10$ GeV in agreement with the typical transverse momentum thresholds imposed by the experiments, and the l^+l^- -mass of j^+ production was chosen at $M_{j^+} = 10$ GeV. At $\sqrt{S} = 540$ GeV, typical cross section values are

$$\sigma(j\bar{j}, Z^0 j, W^+ j) = (10^{-34}; 3.70^{-36}; 10^{-36}) \text{ cm}^2 \quad (6.D)$$

whereas all others are at least one order of magnitude lower. In Fig. 2D.b is exposed the integrated cross section of the 4-parton processes in (3.D)-(5.D). The results reveals that at $\sqrt{S} = 540$ GeV the 4-parton production of two gauge bosons is insignificant, at most a few percent of the analogous 2-parton process. Assuming that W and Z could be identified via their two-jet decay modes with the branching ratio $BR(W \rightarrow jj) \sim 75\%$. It is noticed that the cross section for W^+jj etc. Fig. 1D.e is a substantial background for the signal such as $W^+ + (W^- \rightarrow)jj$.

An increase of \sqrt{S} to 620 GeV, or even very much higher, increases substantially the rates. Whilst going to $\sqrt{S} = 2\text{TeV}$ one may expect a gain of two orders of magnitude in the production of a gauge boson pair and three orders of magnitude for $W+jj$ etc.

Taking into account the possibility of observing experimentally the mechanism under investigation, it becomes worthwhile to analyse it more rigorously and in detail. The simplest and analogous mechanism which can enlighten the structure of the double scattering for instance is the double Drell-Yan annihilation. We shall study this process in the QCD framework in the last section. In the following sections we shall briefly comment on first the single Drell-Yan process and then account for the few available pheomenological considerations on the double Drell-Yan mechanism.

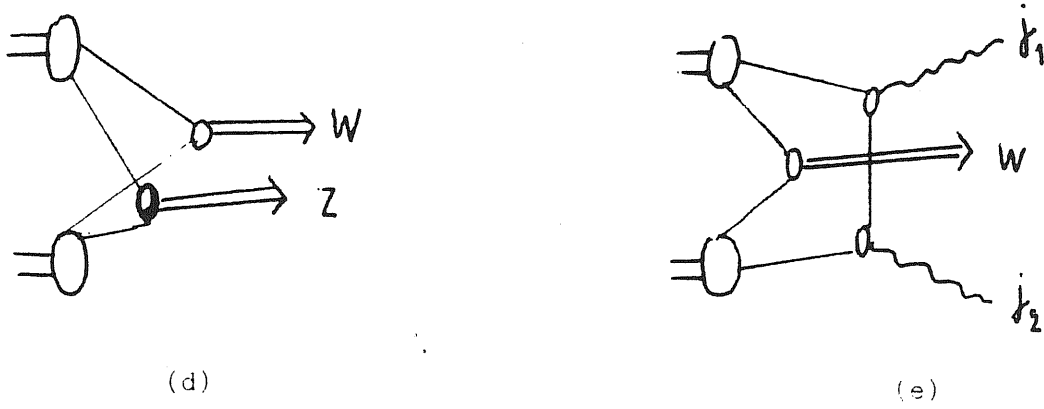
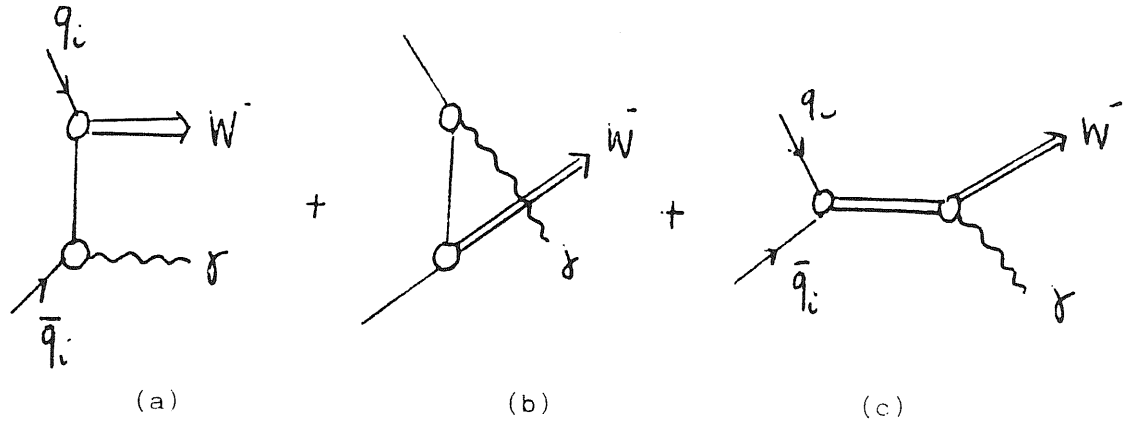
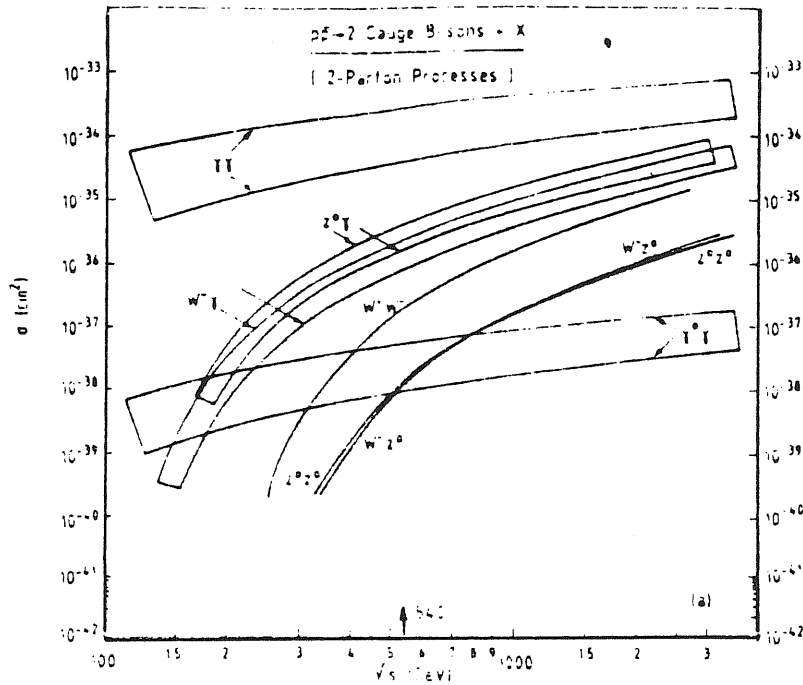
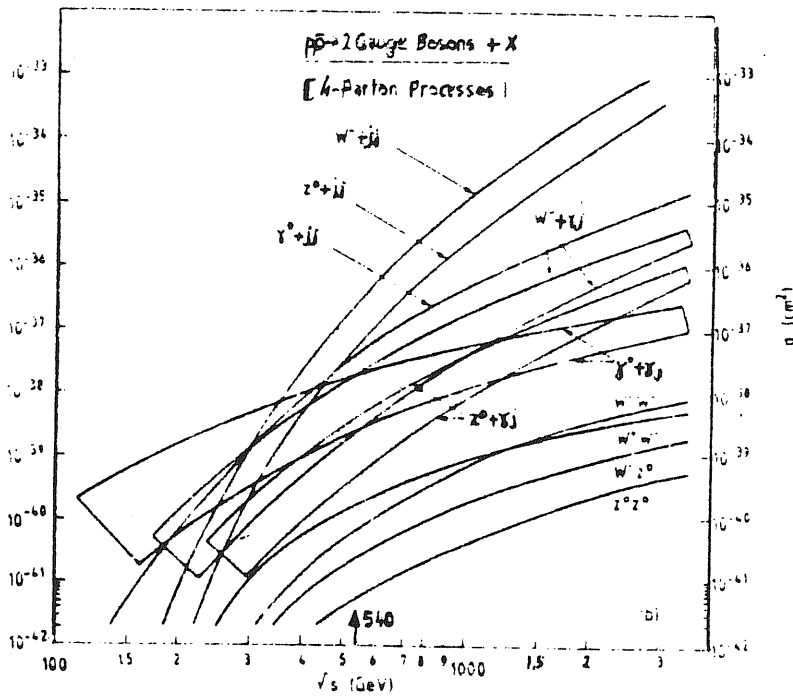


Fig. 1D: a-c) The 2-parton production of gauge boson pairs by the abelian graphs (a), (b) and the non-abelian diagram (c).
d-e) The 4-parton production of a gauge boson pair (d); and one gauge boson with a pair of quark/gluon jets (e) where the mass cut $M_{jj} \geq 70$ GeV is imposed.



(a)



(b)

Fig. 2D: a) The integrated cross section for the 2 parton production of a gauge boson pair with a transverse momentum cut-off: $P_T(\gamma) = 5.10$ GeV for the processes involving a "direct" photon. The Drell-Yan mass is $M^* = 10$ GeV.

b) The integrated cross section for the 4-parton production of a gauge boson pair, one gauge boson with a "direct" photon accompanied by a quark/gluon jet, or one gauge boson and a pair of quark/gluon jets. The transverse momentum cut-off $P_T(\gamma) = 10$ GeV is applied whenever a "direct" photon or a quark/gluon jet is produced $M^* = 10$ GeV.

E. Single and double Drell-Yan mechanism: phenomenological considerations

E1. Single Drell-Yan process in the parton model

The model proposed by Drell and Yan⁽³⁵⁾ to describe the massive lepton pair production in hadron-hadron collisions is depicted in Fig. 1E

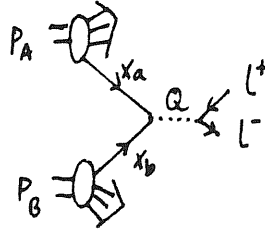


Fig. 1E: Single Drell-Yan mechanism

In this model a quark from one of the incoming hadrons annihilates with the corresponding antiquark from the second hadron producing a virtual photon of mass Q , which then decays into a pair of leptons. For simplicity one usually neglects the transverse momenta of the quarks inside the hadrons and the masses involved. The differential cross section $\frac{d\sigma}{dQ^2}$ in the naive parton model is given by

$$\frac{d\sigma}{dQ^2} = \frac{4\pi\alpha^2}{9Q^2} \sum_{\text{all flavors}} \tau e_q^2 \int dx_a dx_b G_A(x_a) G_B(x_b) \delta(\tau - x_a x_b) + (x_a \leftrightarrow x_b) \quad (1.E)$$

The functions $G_A(x_a)$ and $G_B(x_b)$ represent the probabilities of finding the quark and the antiquark with a fraction x_a and x_b of the parent particle momentum. While the scaling variable $\tau = \frac{Q^2}{s}$ represents the fraction of the total C.M energy used in the formation of the virtual photon. Written in a compact way, the formula (1.E) becomes

$$\frac{d\sigma}{dQ^2} = \frac{4\pi\alpha^2}{9Q^2} F(\tau) \quad (2.E)$$

with
$$F(\tau) = \sum_{\substack{\text{all} \\ \text{flavours}}} \tau e_q^2 \int dx_a dx_b G_{A \rightarrow a}(x_a) G_{B \rightarrow b}(x_b) \delta(\tau - x_a x_b) + (x_a \leftrightarrow x_b). \quad (3.E)$$

Here the scaling functional $F(\tau)$ is formed entirely from the dimensionless variables.

The form of the cross section (2.E) had many phenomenological successes. It predicts the scaling of the cross section that is $F(\tau)$ is independent of S or Q^2 at fixed τ . The best test of scaling existing so far is shown in Fig. 2E. The principal failure, however, of the above picture is incontestably the large transverse momentum of the lepton pair observed experimentally. In the simple Drell-Yan mechanism, the transverse momentum of the virtual photon is related to the transverse momentum of the annihilating quarks. In the parton model, such transverse momentum is related through the uncertainly principal to the size of the parent hadron and is expected to be of the order of about 300 MeV/c. It was therefore a surprise when the observed transverse momentum of the lepton pair was found to be large at large masses and to increase with S .

The Drell-Yan mechanism will recover its validity in the framework of the QCD parton model which introduces modifications to the simple picture of Fig. 1E in the form of the possible emission of gluons.

E2 Single Drell-Yan process in QCD

Quantum chromodynamics introduces modifications to the parton model in the form of the possible emission of gluons.

The first order diagrams in the strong coupling constant α_s , which contribute to the Drell-Yan process are shown in Fig. 3E

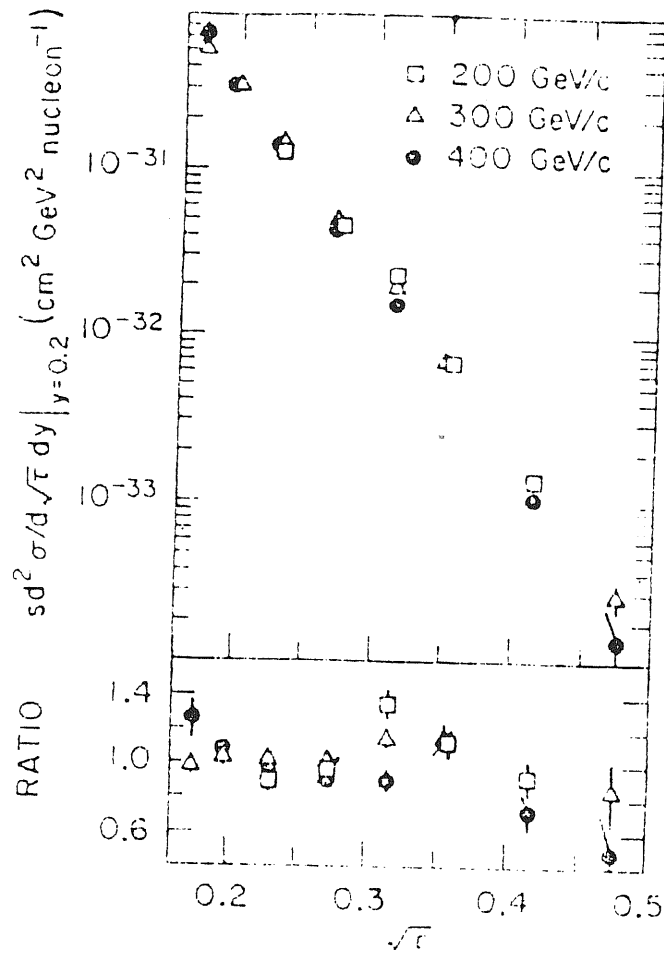


Fig. 2E

Fig. 2E: Scaling function and the corresponding ratios at 200,300 and 400 GeV/c

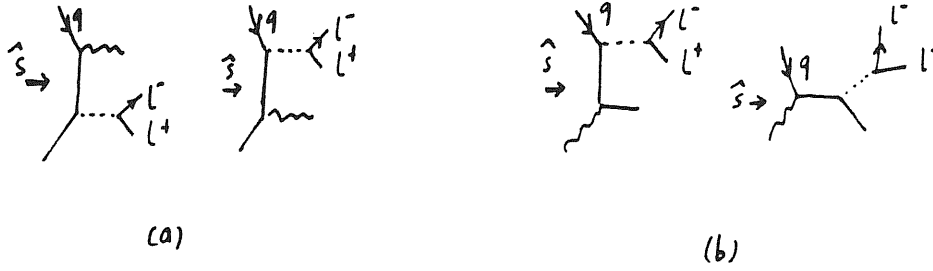


Fig. 3E: a) "Annihilation", b) "Compton", First order in α_s QCD diagrams contributing to the Drell-Yan process

We shall develop in the last part of the present subsection, the one gluon insertion in the single Drell-Yan process in the leading log approximation. The result of it will be used in our analysis of the evolution of the double structure functions in the double Drell Yan process.

Of course, there are many higher order diagrams which contribute less to the cross section due to the higher powers of α_s . These are usually neglected in the phenomenological calculations. The first order diagrams correspond to the "compton" and "annihilation" processes respectively, where the gluon plays the role analogous to the photon in QED. The subprocess variables \hat{s} , \hat{t} , \hat{u} are related to the overall C.M variables through the following set of relations

$$\begin{aligned}
 \hat{s} &= x_a x_b S \\
 \hat{t} &= x_a t + (1-x_a) Q^2 \\
 \hat{u} &= x_b u + (1-x_b) Q^2
 \end{aligned}
 \tag{4.E}$$

Here, the transverse momenta of the quarks and the masses involved has been neglected. Both the "compton" and "annihilation" cross sections can be calculated⁽³⁶⁾ and expressed in terms of the subprocess variables

$$\frac{d\sigma}{dQ^2 d\hat{t}} = \frac{8}{27} \alpha_s^2 e_i^2 \frac{2Q^2 \hat{s} + \hat{u}^2 + \hat{t}^2}{\hat{s}^2 \hat{t} \hat{u}} \quad (\text{annihilation}) \quad (5.E)$$

$$\frac{d\sigma}{dQ^2 d\hat{t}} = \frac{1}{9} \alpha_s^2 e_i^2 \frac{2Q^2 \hat{u} + \hat{s}^2 + \hat{t}^2}{-\hat{s}^2 \hat{u}} \quad (\text{compton}) \quad (6.E)$$

Both formula (5.E) and (6.E) are divergent for the small value of \hat{t} or \hat{u} and therefore are difficult to use in phenomenological applications. Politzer⁽³⁷⁾ and Sachrajda⁽³⁸⁾ have proposed a perturbative approach which includes the first order diagrams in the leading $\log Q^2$ approximation. For $q\bar{q}$ annihilation, Politzer found that the divergent parts of the contributions due to the soft emission have a factorizable form and that they can be absorbed into the incoming particle wave functions. Similar results were obtained by Sachrajda for the quark-quark, quark-gluon and gluon-gluon subprocesses. The structure functions of the parent particle become Q^2 dependent, but they are again the same as in deep inelastic lepton scattering. As a result, the parton model description of the Drell-Yan is recovered but with additional scale violating component, see Fig. 4E. The cross section takes the form

$$\frac{d\sigma}{dQ^2} = \frac{4\pi\alpha^2}{9Q^4} F(\tau, Q^2). \quad (7.E)$$

There are several steps in this approach for which the theoretical understanding is not yet complete.

1 - Diagrams of higher order in α_s contributing to the process also have similar types of divergencies in the cross sections.

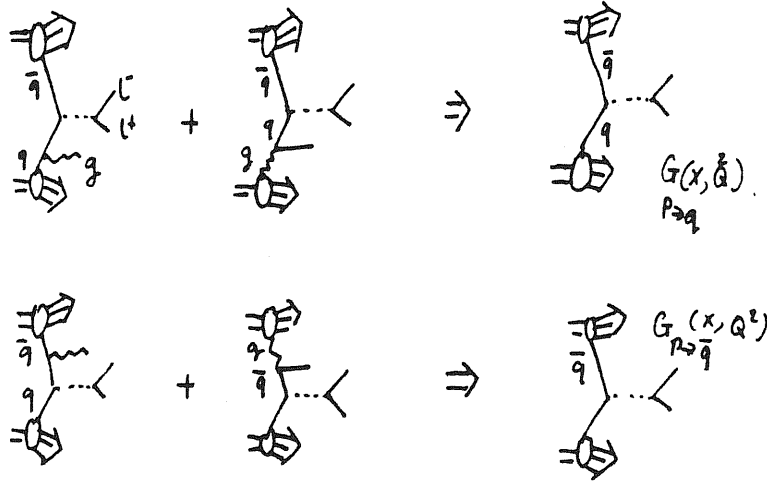


Fig. 4E: Illustration of the diagrams contributing to the renormalization group improved quark and antiquark distributions

Although some second order terms have already been calculated, it is so far not proven that all those divergencies may be treated in the same way as in the case of the first order diagrams.

2 - Non-leading terms, neglected in first approximation, may have substantial contributions to the cross section, thus modifying the results.

3 - The identification of the scale breaking variable Q^2 with the photon mass may not be correct in the kinematical regions of phase space with two or more large dimensional variables, e.g. for large mass lepton pairs produced at high transverse momentum.

E3 QCD phenomenology of single lepton-pair production

Until recently most of the features of the lepton pair data such as beam dependence, scaling, longitudinal momentum distribution etc., were well described by the Drell-Yan parton model. The need for the departure from such a simple picture is, however indicated by the large transverse momentum of the lepton pair. The QCD procedure described in the preceding section was used by several authors^(36,39,40,41)

to calculate the first order diagram predictions for the Drell-Yan process. The calculations required as input the individual quark structure functions. The agreement of such calculations with the measured mass spectra and the longitudinal distributions seems to be quite satisfactory⁽⁴²⁾, thus reproducing the success of the parton model. The transverse momentum distributions require, however, a more complicated approach. In the perturbative QCD the virtual photon acquires its transverse momentum through the emission of hard gluons. The first order in α_s diagrams can be calculated according to formulae (5.E) and (6.E). Their contribution to the total P_T spectrum is shown in Fig. 5E. In the region of small transverse momenta, where both "annihilation" and "compton" contributions diverge, one can argue that the non-perturbative confinement phenomena dominate. Nevertheless, even above $P_T = 1$ GeV/C the contribution of the first order diagrams is about a factor of two smaller and has the curvature opposite to that of the data. This does not mean, however, that the QCD is necessarily failing to describe the Drell-Yan process. There are in the literature several ways of explaining this problem, namely "primordial" transverse momentum, "higher twist" effects, etc.

Independently of the various approaches, it is clear from Fig. 5E that the measurements of the lepton pair production at very large P_T will provide a sensitive test of QCD. In this region the higher order corrections are expected to be negligible and numerical comparisons of the first order calculations with the data will be possible.

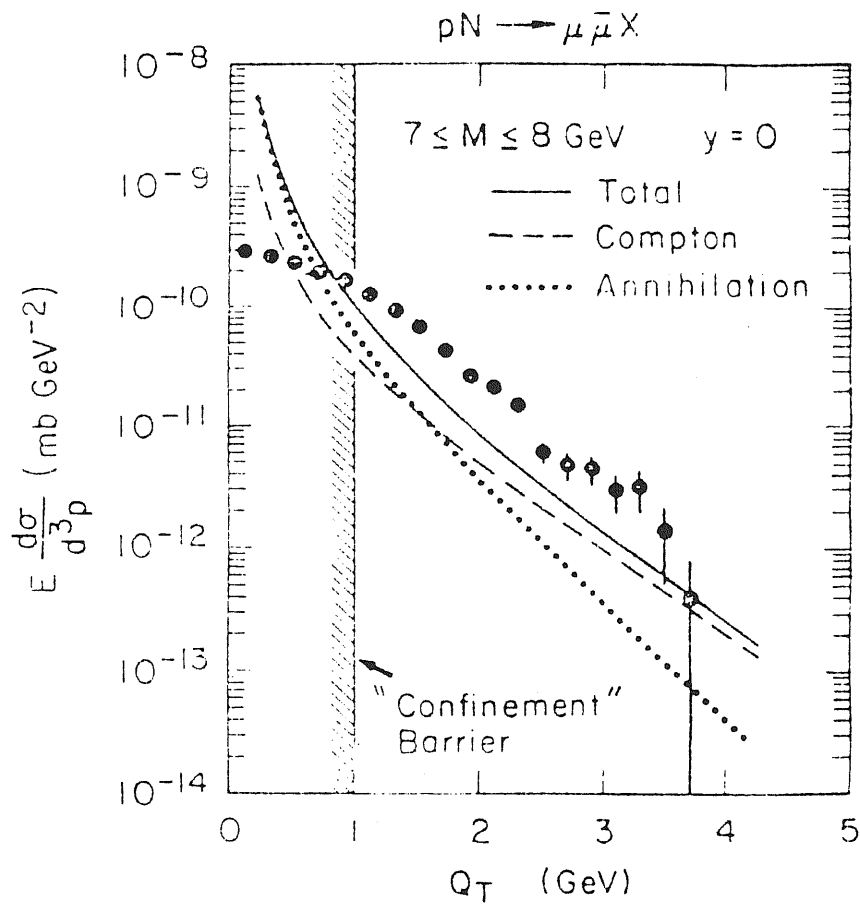


Fig. 5E

Fig. 5E: Comparison of the QCD calculations of dimuon transverse momentum

E4 Diagrammatic analysis of the first order (α_s) contributions in the (LLA) to the single Drell-Yan process

In this subsection we propose to study diagrammatically all the first order diagrams in detail, in the leading logarithm approximation. The set of diagrams to be investigated are the following Fig. 6E.

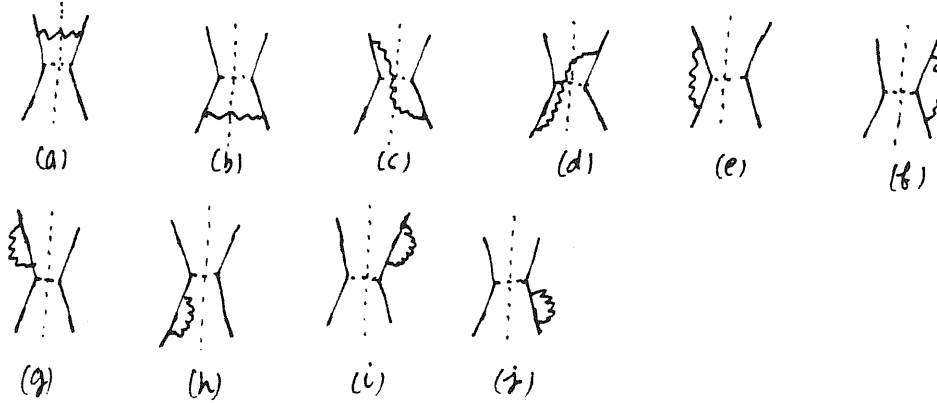


Fig. 6E: All first order (α_s) corrections to the Drell-Yan process. Wavy lines are gluons and dashed lines are massive photons.

I) Infra-red and collinear singularities

1) Real emission

To compute real emission diagrams (a), (b), (c), (d), we adopt the physical gauge ($\epsilon^2 = -1$, $\epsilon \cdot k = \bar{\epsilon} \cdot \bar{k} = 0$; ϵ is the gluon polarization). In this gauge the diagrams (c) and (d) do not contribute to the leading log approximation, while (b) gives an identical contribution to that of (a), therefore we have to compute only the diagram (a) for the real emission.

To set up the kinematics we draw up again the diagram (a)



The contribution to the total cross section of the diagram (a) has the form

$$\sigma = \frac{1}{2S} \cdot \frac{1}{4} \cdot \frac{1}{3} g^2 e^2 C_F \sum_{(spin)} \sum_{(pol)} \frac{\int d^4 k}{(2\pi)^4} 2\pi \delta_+(k^2 - \lambda^2) 2\pi \delta(q^2 - Q^2) \cdot$$

$$\times \frac{\bar{u}(p') \not{\epsilon}_\mu (p-k) \not{\epsilon}_\nu u(p) \bar{u}(p') \not{\epsilon}_\mu (p-k) \not{\epsilon}_\nu u(p)}{t^2} \quad (8.E)$$

where $t = (p-k)^2$, $\delta_+(p^2) = \theta(p_0) \delta(p^2)$ and λ is the photon regularization mass. We use the Sudakov decomposition to parametrise the gluon momentum

$$k = \alpha p' + (1-\beta)p + k_T \quad (9.E)$$

the phase space integral in terms of Sudakov variables α, β, \vec{k}_T reads

$$\int \frac{d^4 k}{(2\pi)^4} 2\pi \delta_+(k^2 - \lambda^2) = \frac{pp'}{8\pi^2} \int d\alpha d\beta d^2 k_T \delta[2\alpha(1-\beta)pp' - k_T^2]$$

$$= \frac{1}{16\pi^2} \int d\beta dt \quad (10.E)$$

Therefore σ takes the form

$$\sigma = -\frac{\alpha_s}{6S} C_F e_q^2 \frac{1}{4} \int d\beta \frac{dt}{t^2} \sum_{(pol)} \frac{\pi}{2} \bar{u}(p') \not{\epsilon}_\mu (p-k) \not{\epsilon}_\nu u(p) \bar{u}(p') \not{\epsilon}_\mu (p-k) \not{\epsilon}_\nu u(p) \delta(q^2 - Q^2) \quad (11.E)$$

We perform the sum over the gluon polarization

$$X = \sum_{(pol)} (p-k)_\mu \not{\epsilon}_\mu (p-k)_\nu \not{\epsilon}_\nu = \sum_{(pol)} 4(p \cdot \epsilon)^2 (p-k)_\mu (p-k)_\mu - 2k^2 + 4(p \cdot \epsilon)(p \cdot k) \not{\epsilon} \quad (12.E)$$

The last term is proportional to $(-t)^{3/2}$ and therefore does not give rise to logarithms after integration over t , while the first and the second do. To sum over the polarization, we use the formula

$$\sum_{(pol)} (p \cdot \epsilon)^2 \simeq -\frac{t}{1-\beta} \quad (13.E)$$

Therefore the quantity X is simply written as

$$X = -2t \frac{1+\beta^2}{\beta(1-\beta)} (p-k). \quad (14.E)$$

Putting this into formula (11.E) we get

$$\sigma = \frac{1}{3\bar{s}} \alpha_s e_q^2 \int \frac{d\beta}{\beta} 2\pi \delta(q^2 - Q^2) \frac{1+\beta^2}{1-\beta} \int_{t_M}^{t_m} \frac{dt}{t} T_2 \gamma p \gamma' (p-k). \quad (15.E)$$

One needs to know the integration bounds t_m and t_M in the case where the gluons have been attributed a small regularization mass. The upper and lower bound t_m and t_M are given by

$$\begin{aligned} t_m &= -\frac{1^2 Q^2}{\bar{s} - Q^2} \\ t_M &= Q^2 \bar{s} \end{aligned} \quad (16.E)$$

The integration over t reads now

$$\int_{t_M}^{t_m} \frac{dt}{t} = \ln \left| \frac{t_m}{t_M} \right| = \ln \frac{1^2 Q^2}{(\bar{s} - Q^2)^2} \simeq \ln \left(\frac{1^2}{Q^2} \right) \quad (17.E)$$

The integral over β is straightforward

$$\int \frac{d\beta}{\beta} \delta(q^2 - Q^2) = \int \frac{d\beta}{\beta} \delta(2\beta p p' - Q^2) = \frac{1}{2\bar{s} p p'} \quad \text{with } \bar{s} = \frac{Q^2}{\bar{s}} \quad (18.E)$$

The trace of γ matrices gives

$$\frac{1}{4} \text{Tr} \not{p}' \gamma^\mu (\not{p} - \not{k}) \gamma_\mu = -2 \not{p} \not{p}' \quad (19.E)$$

where we have put $(\not{p} - \not{k}) \simeq \not{p}$

Thus inserting all these details into the formula (11.E) gives the final result

$$\sigma = 2 \cdot \frac{\pi \alpha_s \alpha}{5} \left(\frac{8}{9}\right) e_q^2 \frac{1 + \hat{s}^2}{1 - \hat{s}^2} \ln \frac{Q^2}{\lambda^2} \quad (20.E)$$

The factor 2 in front is added to account for diagram (b) which gives an equal contribution.

Adding real gluon contributions to the zeroth order we get

$$\sigma = \frac{4\pi^2 \alpha}{3\hat{s}} e_q^2 \left[\delta(1 - \hat{s}) + 2 \cdot \frac{\alpha_s}{2\pi} \frac{4}{3} \frac{1 + \hat{s}^2}{1 - \hat{s}^2} \ln \frac{Q^2}{\lambda^2} + \dots \right] \quad (21.E)$$

Real emission alone is infra-red divergent, this is manifest in the above expression since for $\hat{s} = 1$, the quantity $\frac{1 + \hat{s}^2}{1 - \hat{s}^2}$ diverges. These infinities are cancelled out by virtual emission, so in order to get an infra-red stable result, one has to consider all possible virtual diagrams present at order α_s .

2) Virtual emission

Here we study infra-red and collinear singularities associated with diagrams (e) and (f). This correction to the vertex contains ultraviolet divergences as well as infra-red and collinear ones. The former will be the object of the next subsection.

The collinear divergence along the momentum \vec{p} i.e. $\vec{k} // \vec{p}$ arises from the situation where the disintegration $p \rightarrow k + (p-k)$ is nearly physically realized, i.e. we have

$$k^2 \approx 0 \quad ; \quad (p-k)^2 \approx 0 \quad k^0 > 0 \quad \text{and} \quad (p-k)^0 > 0 \quad (22.E)$$

The case \vec{k}/\vec{p}' is obviously identical to \vec{k}/\vec{p} . It is again useful to use the Sudakov parametrization

$$k = \alpha p' + (1-\beta) p + k_T \quad (23.E)$$

The amplitude corresponding to diagram (e) or (f) is given by

$$A = i g^2 C_F \int \frac{d^4 k}{(2\pi)^4} \frac{\bar{u}(p') \gamma_\rho (p' + k) \gamma_\mu (p - k) \gamma^\rho u(p)}{(k^2 - \lambda^2 + i\varepsilon) [(p+k)^2 + i\varepsilon] [(p-k)^2 + i\varepsilon]} \quad (24.E)$$

we have adopted here the Feynman gauge.

The different terms of the denominator read in terms of α , β , \vec{k}_T

$$\begin{aligned} k^2 - \lambda^2 + i\varepsilon &= 2\alpha(1-\beta)p \cdot p' - k_T^2 - \lambda^2 + i\varepsilon \\ (p-k)^2 + i\varepsilon &= -2\alpha\beta p \cdot p' - k_T^2 + i\varepsilon \\ (p'+k)^2 + i\varepsilon &= 2(1+\alpha)(1-\beta)p \cdot p' - k_T^2 + i\varepsilon \end{aligned} \quad (25.E)$$

The integration over α is different from zero as it should be only if $0 \leq \beta \leq 1$. That is, the different poles do not gather in the same half plane of the complex α variable. For $0 \leq \beta \leq 1$, there is only one pole in the upper half plane

$$\alpha = \frac{-k_T^2 + i\varepsilon}{2\beta p \cdot p'} \quad (26.E)$$

And so we close the contour as sketched below. Fig. 7E

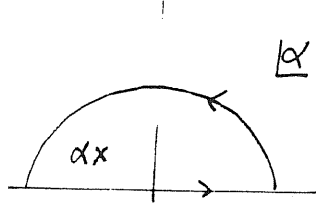


Fig. 7E: Contour of integration in the complex (α) plane

Therefore the integral becomes

$$\frac{\int d^4k}{(k^2 - \lambda^2 + i\epsilon) [(p-k)^2 + i\epsilon]} = \int i\pi^2 \frac{d\beta dk_T^2}{k_T^2 + \beta\lambda^2} \quad (27.E)$$

The logarithmic term will be given by the k_T integration, therefore one can neglect in the numerator all terms proportional to k_T^2 or to α since $\alpha \sim k_T^2$. Thus we just put

$$k \simeq (1-\beta)p \quad (28.E)$$

Now the amplitude A takes the form

$$A_{\vec{k} // \vec{p}} = ig^2 C_F \int \frac{i\pi^2 d\beta dk_T^2}{(2\pi)^4} \frac{\bar{v}(p') \not{K} (\not{p} + \not{k}) \not{\gamma}_\nu u(p)}{(k_T^2 + \beta\lambda^2) (p+k)^2} \frac{2\beta}{1-\beta} \quad (29.E)$$

$A_{\vec{k} // \vec{p}}$ means that we consider only the part of the phase space where \vec{k} is collinear to \vec{p} .

$$A_{\vec{k} // \vec{p}} = -\frac{\alpha_s}{4\pi} C_F \ln\left(\frac{Q^2}{\lambda^2}\right) \int_0^1 d\beta \frac{2\beta}{1-\beta} \bar{v}(p') \not{\gamma}_\nu u(p). \quad (30.E)$$

The contribution of diagram (e) and (f) to the total cross section then reads

$$\sigma = \frac{4\pi\alpha_s^2}{3S} \frac{1}{2} \left[-2 \cdot \frac{\alpha_s G_F}{2\pi} \int_0^1 \frac{d\beta}{1-\beta} d\beta \ln\left(\frac{Q^2}{\lambda^2}\right) \delta(1-\hat{z}) \right]. \quad (31.E)$$

In this result we have taken into account the contribution of the gluons collinear to \vec{p}' ($A_{\vec{k}/\vec{p}'}$) by multiplying the above result by a factor 2.

II) Ultraviolet singularities

1) The renormalized vertex $\Gamma_\nu R$

As it is well known, the vertex correction is ultraviolet divergent. To work out the renormalized part we adopt the Feynman gauge and the dimensional regularization scheme.

In the Feynman gauge, the expression to first order in α_s of the vertex correction reads

$$\Gamma_\nu = i g^2 G_F \mu^{2\epsilon} \int \frac{d^D k}{(2\pi)^D} \frac{\delta_\mu(p'+k) \delta_\nu(p-k) \gamma^\mu}{(k^2 - \lambda^2) (p'+k)^2 (p-k)^2}. \quad (32.E)$$

Here $\epsilon = 2 - D/2$ and we introduce a mass μ , since the coupling constant has a dimension in D-dimension. The denominator has an ultraviolet behaviour of the form k^6 , therefore only terms proportional to k^2 in the numerator give rise to ultraviolet divergence.

The part of the numerator which gives a divergent integral is given by

$$\tilde{N}_\nu = -(2-D) i g^2 k_\mu k_\nu - k^2 \delta_{\mu\nu}. \quad (33.E)$$

We combine the terms in the denominator using the Feynman identity and make the change of variable

$$k \rightarrow k + x_1 p + x_2 p' \quad (34.E)$$

The part of Γ_N corresponding to \tilde{N}_N is simply written

$$\tilde{\Gamma}_N = 2ig^2 C_F \nu^{2\varepsilon} \int_0^\infty dx_1 dx_2 dx_3 \delta(1 - \sum_{i=1}^3 x_i) \int \frac{d^D k}{(2\pi)^D} \frac{(2-D)(k_\mu k_\mu - k_\nu^2)}{[k^2 - R^2(x_i)]^3} \quad (35.E)$$

with $R^2(x_i) = -x_1(1-x_1)p'^2 - x_2(1-x_2)p^2 - x_1 x_2 Q^2 + x_1^2 x_3$.

integrating over k in D dimensions using the substitution

$$k_\mu k_\mu \rightarrow \frac{1}{D} k^2 \gamma_\mu \quad (36.E)$$

Hence $\tilde{\Gamma}_N$ becomes

$$\tilde{\Gamma}_N = \frac{g^2 C_F}{(4\pi)^{D/2}} \nu^{2\varepsilon} \frac{(D-2)^2}{2} \int dx_1 dx_2 dx_3 \delta(1 - \sum_{i=1}^3 x_i) \frac{\Gamma(2-D/2)}{[R^2]^{2-D/2}} \gamma_\mu. \quad (37.E)$$

where we have used the general formula

$$\int \frac{d^D k}{(2\pi)^D} \frac{k^2}{(k^2 - R^2 + i\varepsilon)^N} = \frac{i}{2} \frac{(-)^{N-1}}{(4\pi)^{D/2}} \frac{\Gamma(N-1-D/2)}{\Gamma(N)} \frac{D}{(R^2 - i\varepsilon)^{N-1-D/2}}. \quad (38.E)$$

Developing the expression $\tilde{\Gamma}_N$ around $\varepsilon = 0$ and taken the asymptotic limit $R^2(x_i) \simeq Q^2$, the renormalized quantity Γ_{NR} obtained by subtracting the pole in ε is given by

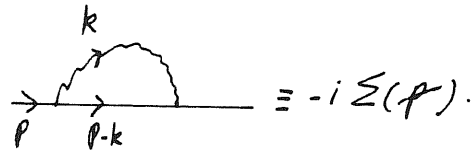
$$\Gamma_{NR} \simeq -\gamma_N \frac{g^2 C_F}{8\pi} \int dx_1 dx_2 dx_3 \delta(1 - \sum_{i=1}^3 x_i) \ln\left(\frac{Q^2}{\mu^2}\right). \quad (39.E)$$

Therefore we get

$$\Gamma_{NR} \simeq -\gamma_N \frac{g^2 C_F}{4\pi} \ln\left(\frac{Q^2}{\mu^2}\right). \quad (40.E)$$

2) The renormalized self-energy $\Sigma_R(p)$.

Let us compute the renormalized self-energy $\Sigma_R(p)$ associated with the diagram



$$\text{Diagram} \equiv -i \Sigma(p).$$

Its expression is given in the Feynman gauge by

$$\Sigma(p) = -ig^2 C_F \mu^{2\epsilon} \int \frac{d^D k}{(2\pi)^D} \frac{\gamma^\mu (\not{p}-\not{k}) \gamma_\mu}{(k^2 \lambda^2)(p-k)^2} \quad (41.E)$$

combining the denominator with the help of the Feynman identity and making the change of variable

$$k \rightarrow k - xp \quad (42.E)$$

we get

$$\begin{aligned} \Sigma(p) &= -ig^2 C_F \mu^{2\epsilon} (2-D) p \int_0^1 dx (1-x) \int \frac{d^D k}{(2\pi)^D} \frac{1}{[k^2 + x(1-x)p^2 - (1-x)\lambda^2]^2} \\ &= -\frac{2}{\epsilon} \frac{\alpha_s C_F}{4\pi} [1 - \epsilon(\gamma - \ln 4\pi)] \int_0^1 dx (1-x) [1 - \epsilon \ln \frac{R^2}{\mu^2}] \end{aligned} \quad (43.E)$$

$$\text{With } R^2 = \lambda^2(1-x) - x(1-x)p^2.$$

neglecting constant terms, $\Sigma(p)$ becomes

$$\Sigma(p) = -\frac{\alpha_s C_F}{4\pi} \frac{p}{\epsilon} + \frac{\alpha_s C_F}{2\pi} p \int_0^1 dx (1-x) \ln \left(\frac{R^2(x)}{\mu^2} \right). \quad (44.E)$$

Now for $p^2=0$ and $\lambda^2 \ll p^2$ the renormalized self energy behaves like

$$\begin{aligned}\Sigma(p) &= \frac{\alpha_s C_F}{4\pi} \ln\left(\frac{p^2}{\mu^2}\right) p \\ &= d\left(\frac{p^2}{\mu^2}\right) p.\end{aligned}\quad (45.E)$$

The renormalized propagator is obtained simply by

$$\frac{i}{p}(-i\Sigma(p))\frac{i}{p} = \frac{i}{p}(-ip d(\frac{p^2}{\mu^2}))\frac{i}{p} = \frac{i}{p} d(\frac{p^2}{\mu^2}). \quad (46.E)$$

Since a propagator is a bilinear expression in the fields, the renormalized wave function is obtained by multiplying the bare wave-function by only $\frac{1}{2}d(\frac{p^2}{\mu^2})$.

Adding the contributions from diagrams (e), (g) and (h) we get

$$\begin{aligned}\sigma &= \frac{4\pi^2\alpha}{3\hat{s}} e_q^2 \delta(1-\hat{z}) \left(\frac{\alpha_s C_F}{4\pi} \ln\frac{p^2}{\mu^2} - \frac{\alpha_s C_F}{4\pi} \ln\frac{Q^2}{\mu^2} \right) \\ &= -\frac{4\pi^2\alpha}{3\hat{s}} e_q^2 \delta(1-\hat{z}) \frac{\alpha_s C_F}{4\pi} \ln\left(\frac{Q^2}{\mu^2}\right).\end{aligned}\quad (47.E)$$

We notice that ultraviolet corrections to the vertex and to the external legs come out equal in absolute value but differ in sign and therefore the renormalization point (μ) disappears in the sum.

So far all radiative corrections to the single Drell-Yan process at the (LLA) are computed. Adding all these contributions we get the expression for the cross section ($q\bar{q} \rightarrow \gamma^*$) at first order in α_s

$$\begin{aligned}\sigma &= \frac{4\pi^2\alpha}{3\hat{s}} e_q^2 \left[\delta(1-\hat{z}) + 2 \cdot \frac{\alpha_s}{2\pi} \cdot \frac{4}{3} \frac{1+\hat{z}^2}{1-\hat{z}} \ln\frac{Q^2}{\lambda^2} - 2 \cdot \frac{\alpha_s}{2\pi} \cdot \frac{4}{3} \int_0^1 \frac{z\beta}{1-\beta} d\beta \delta(1-\hat{z}) \ln\frac{Q^2}{\lambda^2} \right. \\ &\quad \left. - 2 \cdot \frac{\alpha_s}{4\pi} \cdot \frac{4}{3} \ln\frac{Q^2}{\lambda^2} \delta(1-\hat{z}) \right].\end{aligned}\quad (48.E)$$

$$\sigma = \frac{4\pi\alpha^2}{3s} Q^2 \left[\delta(1-\hat{z}) + 2 \cdot \frac{\kappa_s}{2n} \frac{4}{3} \ln \frac{Q^2}{\Lambda^2} \left(\frac{1+\hat{z}^2}{1-\hat{z}} - \int_0^1 \frac{2\beta}{1-\beta} + \frac{1}{2} \right) \delta(1-\hat{z}) \right] \quad (49.E)$$

One can rearrange the above expression using the identity

$$\frac{1}{2} = \int_0^1 \frac{1+\beta^2-2\beta}{1-\beta} d\beta \quad (50.E)$$

Therefore we get

$$\sigma = \frac{4\pi\alpha^2}{3s} Q^2 \left[\delta(1-\hat{z}) + 2 \cdot \frac{\kappa_s}{2n} \frac{4}{3} \ln \frac{Q^2}{\Lambda^2} \left(\frac{1+\hat{z}^2}{1-\hat{z}} \right)_+ \right] \quad (51.E)$$

where $\left(\frac{1+\hat{z}^2}{1-\hat{z}} \right)_+ \equiv \frac{1+\hat{z}^2}{1-\hat{z}} - \int_0^1 \frac{1+\beta^2}{1-\beta} d\beta \delta(1-\hat{z}).$ (52.E)

the distribution $\left(\frac{1+\hat{z}^2}{1-\hat{z}} \right)_+$ is defined by

$$\int \left(\frac{1+\hat{z}^2}{1-\hat{z}} \right)_+ h(\hat{z}) d\hat{z} = \int_0^1 (1+\hat{z}^2) \frac{(h(\hat{z})-h(1))}{1-\hat{z}} d\hat{z} \quad (53.E)$$

The final expression we arrive at and which will be used in the study of the double structure function evolution is given by

$$\sigma = \frac{4\pi\alpha^2}{3s} Q^2 \left[\delta(1-\hat{z}) + 2 \cdot \frac{\kappa_s}{2n} P(\hat{z}) \ln \frac{Q^2}{\Lambda^2} + \dots \right] \quad (54.E)$$

where $P(\hat{z})$ is the Altarelli-Parisi probability

$$P(\hat{z}) = \frac{4}{3} \left[\frac{1+\hat{z}^2}{(1-\hat{z})_+} + \frac{3}{2} \delta(1-\hat{z}) \right]. \quad (55.E)$$

E5 The double Drell-Yan annihilation: phenomenology

The double Drell-Yan mechanism depicted in Fig. 8E has been already studied by the authors of reference (34) for an order of magnitude estimate

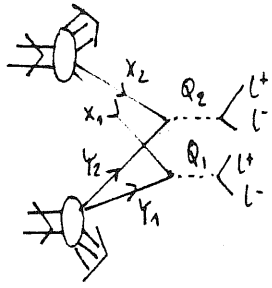


Fig. 8E: The double Drell-Yan mechanism

They propose for the cross section to observe a double pair of mass Q_1 and Q_2 , an expression of the form

$$\frac{d\sigma}{dQ_1 dQ_2} = \frac{1}{\pi R^2} \frac{d\sigma}{dQ_1} \frac{d\sigma}{dQ_2} f(x_1, x_2, y_1, y_2) \quad (56.E)$$

where

$$\frac{d\sigma}{dQ_1 dQ_2} \equiv \left(\frac{d\sigma}{dQ_1 dy_1 dQ_2 dy_2} \right)_{y_1=y_2=0} \quad (57.E)$$

and

$$f(x_1, x_2, y_1, y_2) = \sum_{i_1, i_2} e_{i_1}^2 e_{i_2}^2 G_A(x_1, x_2) G_B(y_1, y_2). \quad (58.E)$$

The summation is over the quark types, e_i is the charge of the quark i , the values of x_i, y_i are fixed at zero rapidities ($y_1=y_2=0$) by

$$x_i = y_i = \frac{Q_i}{\sqrt{s}} \quad \text{and} \quad x_2 = y_2 = \frac{Q_2}{\sqrt{s}} \quad (59.E)$$

The double structure functions $G_A(x_1, x_2)$ and $G_B(y_1, y_2)$ are the same as those introduced in the preceding sections. The transverse distance Δ_T between the two incoming partons which should appear in the definition of the $G_{A,B}$'s is reflected in the factor $\frac{1}{\pi R^2}$. To get an estimate of the cross section (56.E), the authors of reference (34) have parametrized the unknown structure functions as follows

$$\begin{aligned} G_{VV}(x_1, x_2) &= G_{VV}(x_2, x_1) \\ \int_0^{1-x_2} dx_1 G_{VV}(x_1, x_2) &= G_V(x_2) = \frac{A(1-x_2)^n}{\sqrt{x_2}} \\ \int_0^1 dx G_V(x) &= 1 \end{aligned} \quad (60.E)$$

Where G_{VV} denotes the double distribution of the two valence partons in a hadron. A definite result for $G(x_1, x_2)$ is obtained in the limit that hadrons are made up of (identical) valence quarks only. Taking n in Eq. (60.E) to be 1 and 3 for a π meson and a nucleon (N) respectively one gets

$$G_{VV}^N(x_1, x_2) = \frac{7}{8\pi} \frac{(1-x_1-x_2)^{5/2}}{(x_1 x_2)^{1/2}} \quad (61.E)$$

$$G_{VV}^\pi(x_1, x_2) = \frac{3}{2\pi} \frac{(1-x_1-x_2)^{1/2}}{(x_1 x_2)^{1/2}} \quad (62.E)$$

At the valence-quark level Eq. (61.E) is sufficient to determine the cross section in a $p\bar{p}$ interaction. However, πp and pp interactions involve the double distribution of a valence and a sea quark in a nucleon. This distribution can be taken from phenomenological analysis using the recombination model, and probably an adequate guess according to the authors of reference (34) is

$$G_{VS}^N(x_1, x_2) = a G_V(x_1) G_S(x_2) (1-x_1-x_2) \quad (63.E)$$

The constant a can be inferred from the condition

$$\int_0^{1-x_2} dx_1 G_{VS}(x_1, x_2) = G_S(x_2). \quad (64.E)$$

The authors make an order of magnitude estimate and claim that the cross section, though small is accessible with present high intensity π and p beams. They give different rates on a hydrogen target for $Q_1 \sim Q_2 \sim 4$ GeV and incident energy $\sqrt{s} = 27$ GeV, summarized in the following table.

Beam-particle type	Cross section in mb/GeV
\bar{p}	$> 10^{-15}$
π	$> 10^{-17}$
p	$> 5 \cdot 10^{-17}$

So far we developed in detail the existing pheomenology of multiparton disconnected scattering in exclusive as well as inclusive processes. We have shown that such new processes may play an important role at the CERN collider. In the following section we concentrate on the conceptual⁽³⁾ side of the problem, thus analysing the double Drell-Yan annihilation in the QCD framework, pointing out the features of multiparton processes not properly put into evidence, so far by phenomenological considerations.

In this section we investigate double quark-antiquark annihilation as a multiparton process in the framework of Quantum Chromodynamics⁽⁹⁾. The spin and colour structure as well as factorizability of the process will be analysed in detail. The analysis shows that the existence of connecting gluons does not spoil factorizability in the leading-log approximation. We also find that the spin and colour degrees of freedom play an important role in the description of disconnected processes. As a consequence, hadrons are described by a set of six newly defined structure functions, and it is found that these are convoluted with two completely uncorrelated single Drell-Yan cross sections.

\tilde{A}) Formalism of the double scattering

We study in this subsection the amplitude A associated with the diagram in Fig. (1. \tilde{A})

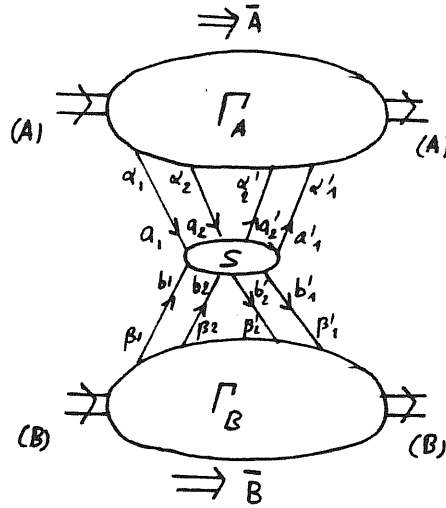


Fig. 1. \tilde{A} : The diagram corresponding to the amplitude A , arrows indicate the momentum flow. The hard blob S is disconnected (up to radiative corrections).

There are six independent internal momentum variables, we choose them as $\sigma, \Sigma, \bar{A}, \bar{B}, \sigma', \Sigma'$ with

$$\begin{aligned}\sigma &= \frac{a_1 - a_2}{2} \\ \Sigma &= \frac{b_1 - b_2}{2} \\ \sigma' &= \frac{a'_1 - a'_2}{2} \\ \Sigma' &= \frac{b'_1 - b'_2}{2}\end{aligned}\quad (1.\tilde{A})$$

The amplitude A according to Fig. (1. \tilde{A}) can be written as (the α 's are Dirac indices, colour indices are understood for the moment).

$$A = \int \frac{d\sigma}{(2\pi)^4} \frac{d\Sigma}{(2\pi)^4} \frac{d\bar{A}}{(2\pi)^4} \frac{d\bar{B}}{(2\pi)^4} \frac{d\sigma'}{(2\pi)^4} \frac{d\Sigma'}{(2\pi)^4} \Gamma_{A, \alpha_1 \alpha_2 \alpha'_1 \alpha'_2}(\sigma, \bar{A}, \sigma') \int \frac{\beta_1 \beta_2 \beta'_1 \beta'_2}{\alpha_1 \alpha_2 \alpha'_1 \alpha'_2} \Gamma_{B, \beta_1 \beta_2 \beta'_1 \beta'_2}(\Sigma, \bar{B}, \Sigma'). \quad (2.\tilde{A})$$

The disconnected hard amplitude S possesses an extra delta function which we factorize so that S takes on the following form:

$$\int_{\alpha_1, \alpha_2, \dots}^{\beta_1, \beta_2, \dots} \Gamma(\sigma, \Sigma, \bar{A}, \bar{B}, \sigma', \Sigma') = \int_{\alpha_1, \alpha_2, \dots}^{\beta_1, \beta_2, \dots} \Gamma(\sigma, \Sigma, \bar{A}, \bar{B}, \sigma', \Sigma') (2\pi)^4 \delta^{(4)}(\sigma + \Sigma - \sigma' - \Sigma'). \quad (3.\tilde{A})$$

To define the longitudinal fractions of momenta carried by the partons of hadron A, we introduce the light-like four vector η_A in terms of which we write the Sudakov decomposition.

$$\sigma_\nu = x p_\nu + \frac{\sigma_\perp^2 \sigma_T^2}{2x} \eta_{A\nu} + \sigma_{T\nu} \quad (4.\tilde{A})$$

with

$$p_A^2 \simeq \eta^2 = \eta_A \cdot \sigma = p_A \cdot \sigma_T = 0 \quad ; \quad p_A \cdot \eta_A \simeq 1.$$

One can take for η_A for instance $\eta_A \approx \frac{P_B}{P_A \cdot P_B}$
 Similarly:

$$\begin{aligned}\Sigma_N &= \gamma P_{B_N} + \frac{\Sigma^2 + \Sigma_T^2}{2\gamma} \eta_{B_N} + \Sigma_{T_N} \\ \bar{A}_N &= \chi_A P_{A_N} + \frac{\bar{A}_+^2 + \bar{A}_T^2}{2\chi_A} \eta_{A_N} + \bar{A}_{T_N} \\ \bar{B}_N &= \chi_B P_{B_N} + \frac{\bar{B}_+^2 + \bar{B}_T^2}{2\chi_B} \eta_{B_N} + \bar{B}_{T_N}\end{aligned} \quad (5.\tilde{A})$$

and the same for primed variables σ', Σ' . Here $\eta_B \approx \frac{P_A}{P_A \cdot P_B}$. We write the delta function (3. \tilde{A}) as

$$\begin{aligned}\delta^{(4)}(\sigma + \Sigma - \sigma' - \Sigma') &= \delta^{(2)}\left(\sigma_T + \frac{\Sigma}{T} - \sigma'_T - \frac{\Sigma'}{T}\right) \delta(\chi P_{A_+} - \chi' P_{A_+}) \delta(\gamma P_{B_-} - \gamma' P_{B_-}) \\ &= \frac{1}{S} \delta^{(2)}\left(\sigma_T + \frac{\Sigma}{T} - \sigma'_T - \frac{\Sigma'}{T}\right) \delta(x - x') \delta(y - y')\end{aligned} \quad (6.\tilde{A})$$

where \sqrt{S} is the centre of mass energy and $P_{A_+} P_{B_-} \approx S$. The transverse component $\delta^{(2)}\left(\sigma_T + \frac{\Sigma}{T} - \sigma'_T - \frac{\Sigma'}{T}\right)$ mixes the upper and lower parts and it is singular for collinear interacting partons.

In order to achieve factorization of the upper, middle and lower parts, we use the integral representation of the δ -function

$$\delta^{(2)}\left(\sigma_T + \frac{\Sigma}{T} - \sigma'_T - \frac{\Sigma'}{T}\right) = \int e^{-i\Delta_T \cdot (\sigma_T + \frac{\Sigma}{T} - \sigma'_T - \frac{\Sigma'}{T})} \frac{d^2 \Delta_T}{(2\pi)^2} \quad (7.\tilde{A})$$

The parameter Δ_T , being the coordinate conjugate to the relative transverse momentum σ_T for instance, is interpreted as the relative transverse distance, within the hadron, which separates the two incoming partons. This Δ_T dependence is a characteristic of disconnected processes.

Since the hard amplitude $\sum_{\alpha_1, \alpha_2, \dots} \hat{\beta}_1 \beta_2 \dots$ is no longer singular in the collinear direction, one can Taylor expand it around

$x_{A\nu}, y_{B\nu}, x_{\bar{A}\nu}, x'_{A\nu}, y'_{B\nu}, y_{\bar{B}\nu}, p_{B\nu}$, thus

$$\sum_{\alpha_1, \alpha_2, \dots} \hat{\beta}_1 \beta_2 \dots (\sigma, \bar{\sigma}, \bar{A}, \bar{B}, \sigma', \bar{\sigma}') = \sum_{\alpha_1, \alpha_2, \dots} \hat{\beta}_1 \beta_2 \dots (x, y, x_{\bar{A}}, y_{\bar{B}}, p_A, p_B) + \frac{\partial}{\partial \sigma_{\nu}} \sum_{\alpha_1, \alpha_2, \dots} \hat{\beta}_1 \beta_2 \dots (\sigma_{\nu} - x_{A\nu}) + \dots \quad (8.\tilde{A})$$

We shall retain only the first term of the expansion which depends solely on the X-components of the parton's momenta. The remaining terms correspond to higher power corrections in $\frac{1}{S}^{(4)}$. To integrate over the off-shellness and the transverse momenta of the incoming partons, keeping the X-components fixed, we introduce the identity

$$\int d\sigma^4 = \int d\sigma^4 dx \delta(x \cdot \sigma \eta_A). \quad (9.\tilde{A})$$

and similarly for the other variables. Therefore the amplitude A in Eq. (2. \tilde{A}) takes on the form

$$A = \frac{1}{S} \int dx_1 dx_2 dy_1 dy_2 d\bar{\Delta}_T \Gamma_{A, \alpha_1, \alpha_2, \dots}^{(x_1, x_2, \bar{\Delta}_T, \eta_A, p_A)} \sum_{\alpha_1, \alpha_2, \dots} \hat{\beta}_1 \beta_2 \dots (x_1, x_2, y_1, y_2, p_A, p_B) \Gamma_{B, \beta_1, \beta_2, \dots}^{(y_1, y_2, \bar{\Delta}_T, \eta_B, p_B)} \quad (10.\tilde{A})$$

where

$$\Gamma_{A, \alpha_1, \alpha_2, \dots}^{(x_1, x_2, \dots)} = 2\pi \left(\frac{d\sigma}{(2\pi)^4} \frac{d\bar{A}}{(2\pi)^4} \frac{d\sigma'}{(2\pi)^4} \delta(x \cdot \sigma \eta_A) \delta(x \cdot \bar{A} \eta_A) \delta(x \cdot \sigma' \eta_A) \right. \\ \left. \times \Gamma_{A, \alpha_1, \alpha_2, \dots}^{(\sigma, \bar{A}, \sigma')} e^{-i \frac{\Delta}{T} (\sigma \cdot \sigma')} \right)$$

(11. \tilde{A})

and similarly for $\Gamma_{B, \beta_1, \beta_2, \dots}^{(y_1, y_2, \dots)}$. The integrations over X' and Y' have been performed using the last delta function in Eq. (6. \tilde{A}) and we have converted in formula (10. \tilde{A}) to the variables X_1, X_2 and Y_1, Y_2 which

are the momentum fractions corresponding respectively to a_1, a_2 and b_1, b_2 in Fig. 1. \tilde{A} . The total cross section is obtained from the amplitude A by the formula

$$\sigma_D = \frac{1}{2s} \text{Disc}_{(s)} A. \quad (12.\tilde{A})$$

Taking the discontinuity of A in the variable S , the cross section reads

$$\sigma_D = \frac{1}{2s^2} \int dx_1 dx_2 dy_1 dy_2 \int_T d\tilde{A} \tilde{\Gamma}_A(x_1, x_2, \tilde{A}, \dots) \text{Disc}_{(s)} \hat{S}^{\beta\beta'} \tilde{\Gamma}_B(y_1, y_2, \tilde{A}, \dots). \quad (13.\tilde{A})$$

where $\tilde{\Gamma}_A(x_1, x_2, \dots)$ is a cut amplitude in the variable \tilde{A}^2 and similarly for $\tilde{\Gamma}_B$ where the variable is \tilde{B}^2 . The discontinuity in the hard amplitude S is taken over $\hat{S} = (x_1 + x_2)(y_1 + y_2)S$. It has been shown by the authors of Ref. (7) in the rather simple case of colourless and spinless quarks, that one recovers the parton model picture from Eq. (13. \tilde{A}), thus allowing the identification of $x_1 x_2 \tilde{\Gamma}_A(x_1, x_2, \dots)$ in that case as the appropriate structure function up to a normalization constant. We shall not prove it again here but rather concentrate on the generalization of this result to the case when the quarks carry spin and colour degrees of freedom.

a) The spin structure of the cut amplitude $\tilde{\Gamma}_{\alpha_1 \alpha_2 \alpha'_2 \alpha'_1}$

In order to investigate the spin structure of Eq. (13.A) one has to expand the tensor $\tilde{\Gamma}_{\alpha_1 \alpha_2 \alpha'_2 \alpha'_1}$ in the basis of the 16- γ matrices for each pair of indices $(\alpha_1 \alpha_2)$ and $(\alpha'_1 \alpha'_2)$. For massless quarks and to leading order in $\frac{1}{s}$, we have the general expansion

$$\begin{aligned} \tilde{F}_{\alpha_1 \alpha_2 \alpha'_1 \alpha'_2} (x_1, x_2, p, \eta, \Delta) = & G_D \frac{p}{\alpha_1 \alpha'_1} \frac{p}{\alpha_2 \alpha'_2} + G_E \frac{p}{\alpha_1 \alpha'_1} \frac{p}{\alpha_2 \alpha'_2} + G_{D5} (p \delta_5)_{\alpha_1 \alpha'_1} (p \delta_5)_{\alpha_2 \alpha'_2} \\ & + G_{E5} (p \delta_5)_{\alpha_1 \alpha'_1} (p \delta_5)_{\alpha_2 \alpha'_2} + \text{higher order corrections} \end{aligned} \quad (14. \tilde{A})$$

Terms proportional to Δ_T as well as η -terms are not leading⁽⁴⁾, since $\dim \Delta_T = \dim \eta = -1$, also there is only an even number of δ_5 matrices, due to partial conservation. It might appear at first sight that the four tensors are independent. This is not so; to see it, one converts to the helicity basis using the identities

$$\frac{p}{\alpha_1 \alpha'_1} = \sum_{\lambda \lambda'} \delta_{\lambda \lambda'} \frac{1}{\alpha_1} \psi_{\alpha_1} (p, \lambda) \bar{\psi}_{\alpha'_1} (p, \lambda') \quad (15. \tilde{A})$$

and $(p \delta_5)_{\alpha_1 \alpha'_1} = \sum_{\lambda \lambda'} \lambda \delta_{\lambda \lambda'} \frac{1}{\alpha_1} \psi_{\alpha_1} (p, \lambda) \bar{\psi}_{\alpha'_1} (p, \lambda') .$

The quantum number λ is twice the helicity and takes on the values $\lambda = \pm 1$. Therefore \tilde{F} takes on the form

$$\begin{aligned} \tilde{F}_{\alpha_1 \alpha_2 \alpha'_1 \alpha'_2} = & \sum_{\lambda \lambda'} [G_D \delta_{\lambda_1 \lambda'_1} \delta_{\lambda_2 \lambda'_2} + G_E \delta_{\lambda_1 \lambda'_1} \delta_{\lambda_2 \lambda'_2} + G_{D5} \lambda_1 \lambda_2 \delta_{\lambda_1 \lambda'_1} \delta_{\lambda_2 \lambda'_2} \\ & + G_{E5} \lambda_1 \lambda_2 \delta_{\lambda_1 \lambda'_1} \delta_{\lambda_2 \lambda'_2}] \frac{1}{\alpha_1} \psi_{\alpha_1} (x_1 p, \lambda_1) \psi_{\alpha_2} (x_2 p, \lambda_2) \bar{\psi}_{\alpha'_1} (x_1 p, \lambda'_1) \bar{\psi}_{\alpha'_2} (x_2 p, \lambda'_2). \end{aligned} \quad (16. \tilde{A})$$

Now the four tensors in formula (16. \tilde{A}) are not all independent. They are related by the identity

$$(1 + \lambda_1 \lambda_2) \delta_{\lambda_1 \lambda'_1} \delta_{\lambda_2 \lambda'_2} = (1 - \lambda_1 \lambda_2) \delta_{\lambda_1 \lambda'_2} \delta_{\lambda_2 \lambda'_1} . \quad (17. \tilde{A})$$

The quantities G_D, G_E, G_{D5}, G_{E5} are however not all positive definite. In order to write \tilde{F} in terms of well-defined structure function, we express the above mentioned tensors in terms of the following projectors.

$$P_{(1+), 1- \rangle} ; P_{(1+ \rangle + 1- \rangle)} ; P_{(1+ \rangle - 1- \rangle)} . \quad (18. \tilde{A})$$

which are respectively the projectors on the subspace spanned by the states $(1++)$, $1-- \rangle$, on the state $\frac{1+ \rangle + 1- \rangle}{\sqrt{2}}$ and $\frac{1+ \rangle - 1- \rangle}{\sqrt{2}}$. These are the irreducible states of the tensorial space $|1,1_2\rangle = |1,1\rangle \otimes |1_2\rangle$. The matrix elements of the above projectors are given by

$$\begin{aligned} \langle 1,1_2 | P_{(1+), 1- \rangle} | 1'_1, 1'_2 \rangle &= \delta_{1,1'_1} \delta_{1_2, 1'_2} \frac{(1+1,1_2)}{2} \\ \langle 1,1_2 | P_{(1+ \rangle + 1- \rangle)} | 1'_1, 1'_2 \rangle &= \frac{\delta_{1,1'_1} \delta_{1_2, 1'_1} - 1,1_2 \delta_{1,1'_1} \delta_{1_2, 1'_2}}{2} \\ \langle 1,1_2 | P_{(1+ \rangle - 1- \rangle)} | 1'_1, 1'_2 \rangle &= \frac{\delta_{1,1'_1} \delta_{1_2, 1'_2} - \delta_{1,1'_2} \delta_{1_2, 1'_1}}{2} \end{aligned} \quad (19. \tilde{A})$$

One may invert the above expressions (19. \tilde{A}) and write down the tensors of Eq. (16. \tilde{A}) in terms of the three independent projectors. Thus one can write down the cut amplitude $\tilde{\Gamma}_{\alpha_1 \alpha_2 \dots}$ in terms of the above projectors.

$$\begin{aligned} \tilde{\Gamma}_{\alpha_1 \alpha_2 \alpha'_1 \alpha'_2} (x_1, x_2, \dots) &= K \sum_{\lambda \lambda'} \left[\frac{1}{2} G_1 \langle 1,1_2 | P_{(1+), 1- \rangle} | 1,1_2 \rangle + G_2 \langle 1,1_2 | P_{(1+ \rangle + 1- \rangle)} | 1'_1, 1'_2 \rangle \right. \\ &\quad \left. + G_3 \langle 1,1_2 | P_{(1+ \rangle - 1- \rangle)} | 1'_1, 1'_2 \rangle \right] u_{\alpha_1} u_{\alpha_2} \bar{u}_{\alpha'_1} \bar{u}_{\alpha'_2} . \end{aligned} \quad (20. \tilde{A})$$

The normalization factor K and the factor $\frac{1}{2} (\text{Tr } P_{(1+), 1- \rangle}) = 2$ are introduced in such a way that G_b 's are the probabilities to find two quarks within the proton in the helicity state $|b\rangle$ corresponding to the projector $P_{(b)}$.

The structure functions G_b 's ($b=1,2,3$) being now properly defined, one can use the matrix elements (19. \tilde{A}) and performs the summation over the helicities to recover a well-defined expansion in p

and $P\delta_5$. Thus we arrive at the final expansion of the tensor on the physical basis for Dirac indices.

$$\begin{aligned} \tilde{\Gamma}_{\alpha_1 \alpha_2 \alpha'_1 \alpha'_2} (x_1, x_2, \Delta, P) = & K \left[\frac{1}{4} G_1 \left(\frac{P}{\alpha_1 \alpha'_1} \frac{P}{\alpha_2 \alpha'_2} + (P\delta_5)_{\alpha_1 \alpha'_1} (P\delta_5)_{\alpha_2 \alpha'_2} \right) \right. \\ & + \frac{1}{2} G_2 \left(\frac{P}{\alpha_1 \alpha'_2} \frac{P}{\alpha_2 \alpha'_1} - (P\delta_5)_{\alpha_1 \alpha'_1} (P\delta_5)_{\alpha_2 \alpha'_2} \right) \\ & \left. + \frac{1}{2} G_3 \left(\frac{P}{\alpha_1 \alpha'_1} \frac{P}{\alpha_2 \alpha'_2} - (P\delta_5)_{\alpha_1 \alpha'_2} (P\delta_5)_{\alpha_2 \alpha'_1} \right) \right]. \end{aligned} \quad (21.\tilde{A})$$

Now going back to the formula for the cross section σ_D Eq. (13. \tilde{A}) and inserting the expansion (21. \tilde{A}) we get an expression which can be written in a matrix form.

$$\sigma_D = \int dx_1 dx_2 dY_1 dY_2 d\Delta_7^2 G_A^+(x_1, x_2, \Delta) \tilde{\sigma} G_B(Y_1, Y_2, \Delta_7). \quad (22.\tilde{A})$$

where $G_A^+ \equiv (G_{A1}, G_{A2}, G_{A3})$, similarly for G_B , and $\tilde{\sigma}$ is a 3 by 3 matrix

$$\tilde{\sigma} = \begin{pmatrix} \tilde{\sigma}_{11} & \tilde{\sigma}_{12} & \tilde{\sigma}_{13} \\ \tilde{\sigma}_{21} & \tilde{\sigma}_{22} & \tilde{\sigma}_{23} \\ \tilde{\sigma}_{31} & \tilde{\sigma}_{32} & \tilde{\sigma}_{33} \end{pmatrix} \quad (23.\tilde{A})$$

The components $\tilde{\sigma}_{\alpha\alpha'}$ are linear combinations of the elementary cross sections* $\sigma_{DD}; \sigma_{EE}; \sigma_{DE}; \sigma_{ED}$ for instance

$$\begin{aligned} \tilde{\sigma}_{11} &= 2\sigma_{DD} \\ \tilde{\sigma}_{22} &= 4(\sigma_{DD} + \sigma_{EE} - \sigma_{ED} - \sigma_{DE}) \\ \tilde{\sigma}_{12} &= 2(2\sigma_{DE} - \sigma_{DD}). \end{aligned} \quad (24.\tilde{A})$$

* Here D refers to the direct term and E to the exchange one.

The cross sections $\sigma_{KL}(K, L = D, E)$ are the elementary cross-sections associated with definite helicity diagrams. We sketch in Fig. 2.Ã, for a particular colour projection, the four helicity diagrams corresponding to different helicity projections. In these diagrams the loops with arrows indicate the helicity flow.

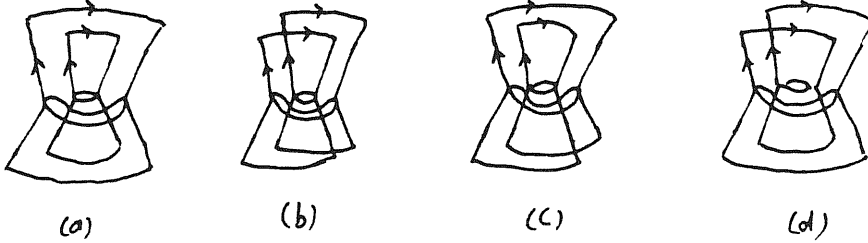


Fig. 2.Ã: The four helicity projections defining the cross-sections σ_{KL}^{IJ} ; $a \equiv \sigma_{DD}^{IJ}$, $b \equiv \sigma_{EE}^{IJ}$, $c \equiv \sigma_{DE}^{IJ}$, $d \equiv \sigma_{ED}^{IJ}$ where the loops indicate the helicity flow.

b) The colour structure of the cut amplitude $\tilde{F}^{i_1 i_2 i'_2 i'_1}$.

Here the indices (i) are colour indices and Dirac indices are understood. The cut amplitude has the following form

$$\tilde{F}^{i_1 i_2 i'_2 i'_1} = \sum_n \bar{\psi}_{i'_1 i'_2}^{(\eta)} \psi_{i_1 i_2}^{(\eta)} = \sum_n \langle P, \bar{n} | i'_1 i'_2 \rangle \langle i_1 i_2 | P, n \rangle \quad (25. \tilde{A})$$

In this notation, we keep only the colour indices and omit all the remaining quantum numbers. η (\bar{n}) refers to the spectator (anti-spectator) system. The quarks belong to the 3-dimensional representation of SU(3) and since $3 \otimes 3 = \bar{3} \oplus 6$, one can expand the two quark state $|i_1 i_2\rangle$ in the irreducible basis $|\bar{3}\rangle$, $|6\rangle$ i.e.

$$|i_1 i_2\rangle = \sum_{a=\bar{3}, 6} \langle a | i_1 i_2 \rangle |a\rangle \quad (26. \tilde{A})$$

Therefore the cut amplitude takes on the following form

$$\tilde{F}^{i_1 i_2 i'_1 i'_2} = \sum_{a=\bar{3}, 6} \sum_{i, i'} \tilde{G}^a \langle i_1 i_2 | a \rangle \langle a | i'_1 i'_2 \rangle. \quad (27. \tilde{A})$$

Since $\tilde{F}^{i_1 i_2 i'_1 i'_2}$ is a colour singlet, only the projectors on the state $|\bar{3}\rangle$ and $|6\rangle$ appear in the sum. To rewrite \tilde{F} with normalized G^a 's we divide the projectors by their traces. Then we arrive at

$$\tilde{F}^{i_1 i_2 i'_1 i'_2} = \frac{2}{N^2 N} G^1 \langle i_1 i_2 | P_{(\bar{3})} | i'_1 i'_2 \rangle + \frac{2}{N^2 N} G^2 \langle i_1 i_2 | P_{(6)} | i'_1 i'_2 \rangle. \quad (28. \tilde{A})$$

with N the number of colour, $N=3$ for $SU(3)$. here G^1 and G^2 stand respectively for the probability to find two quarks within the proton in the colour states $|\bar{3}\rangle$ and $|6\rangle$ and $P_{(\bar{3})}$, $P_{(6)}$ are their corresponding projectors. Their matrix elements are given by the following expressions

$$\begin{aligned} \langle i_1 i_2 | P_{(\bar{3})} | i'_1 i'_2 \rangle &= \frac{\delta_{i_1 i'_1} \delta_{i_2 i'_2} - \delta_{i_1 i'_2} \delta_{i_2 i'_1}}{2} \\ \langle i_1 i_2 | P_{(6)} | i'_1 i'_2 \rangle &= \frac{\delta_{i_1 i'_1} \delta_{i_2 i'_2} + \delta_{i_1 i'_2} \delta_{i_2 i'_1}}{2} \end{aligned} \quad (29. \tilde{A})$$

Now putting the spin and the colour all together we get six independent structure functions $G_b^c(x_1, x_2, \Delta_T)$ ($c=1,2$; $b=1,2,3$) which are the probabilities to find two quarks within the proton in the helicity state ($||++\rangle$ or $|--\rangle$); $\frac{|+-\rangle + |-+\rangle}{\sqrt{2}}$ or $\frac{|+-\rangle - |-+\rangle}{\sqrt{2}}$ and in the colour state $|\bar{3}\rangle$ or $|6\rangle$.

Finally the cross section σ_D takes on the form

$$\sigma_D = \int dx_1 dx_2 d\gamma_1 d\gamma_2 d\Delta_T G_A^+(x_1, x_2, \Delta_T) \tilde{\sigma} G_B^-(\gamma_1, \gamma_2, \Delta_T). \quad (30. \tilde{A})$$

with $G_A^+ = (G_{A1}^1, G_{A1}^2, G_{A2}^1, G_{A2}^2, G_{A3}^1, G_{A3}^2)$ and $\tilde{\sigma}_{\alpha\alpha'}^{ii'}(\alpha, \alpha'=1,2,3; i=i'=1,2)$

is a 6 by 6 matrix generalizing that of Eq. (23.Ä). The upper indices in both $\tilde{\sigma}_{\alpha\beta}^{IJ}$ and G_b^c refer to colour and the lower ones to spin. These cross sections are linear combinations of the elementary cross sections σ_{KL}^{IJ} (I,J,K,L = D,E) generalizing those introduced in Eq. (24.Ä). They correspond to definite colour and helicity diagrams. For a given helicity projection e.g. σ_{DD}^{II} , the cross sections are sketched in Fig. 2.Ä where now the loops indicate the colour flow.

So far the spin and colour analysis leading to formula (30.Ä) is quite general and $\tilde{\sigma}$ may describe any hard disconnected process (e.g. double Drell-Yan, double scattering and so on), so there is a set of structure functions and a set of hard cross sections to compute in order to write down a hadronic cross section. Until now all the attempts to evaluate the double scattering cross section limit themselves to the direct term and this amounts to considering only the component σ_{DD}^{DD} represented in Fig. (2.Äa), all the exchange terms represented by the remaining components are neglected. This is valid of course only for an order of magnitude estimate. We shall see in the next section that the basis in spin and colour on which we have expanded \tilde{F} diagonalizes the matrix $\tilde{\sigma}$ for the double Drell-Yan process. We also show that all the components σ_{KL}^{IJ} can be expressed in terms of the direct one, i.e. σ_{DD}^{DD} and furthermore that σ_{DD}^{DD} factorizes as $\sigma_{DD}^{DD} = \sigma_1 \sigma_2$ where σ_1 and σ_2 are the cross sections for two uncorrelated single Drell-Yan processes.

Ä) Application to the double Drell-Yan process

a) Limited phase space of the connecting gluons in double Drell-Yan mechanism

Here we want to show an important feature of connecting gluons (see Fig. (1.Ä) in the double Drell-Yan (Fig. 2.Ä), namely that in a given diagram the sum of their transverse momentum components

$$k_T = \sum_i k_{Ti} \quad (1.\tilde{B})$$

is always limited and of order $\frac{1}{R}$, where R is the hadronic size. The above statement is trivial and purely kinematical. As can be seen for instance by inspection of Fig. 3B. Momentum conservation requires

$$k_T = q_{1T} + b_{1T} - a'_{1T} - b'_{1T} \quad (2.\tilde{B})$$

Therefore since a_{1T} , a'_{1T} and b_{1T} , b'_{1T} are limited by the hadronic wave functions, k_T must be of the order of magnitude $\frac{1}{R}$. The importance of the above statement comes from the fact that the leading contributions of connecting gluons is just a constant term as we shall see, so at ($\mathcal{L}A$) one could just ignore them with respect to non-connecting gluons to any order in α_s

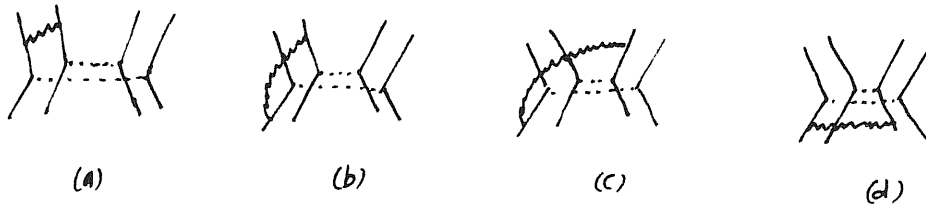


Fig. 1B: The four different types of connecting gluons to order α_s . Gluons are represented by wavy lines, dashed lines correspond to massive photons

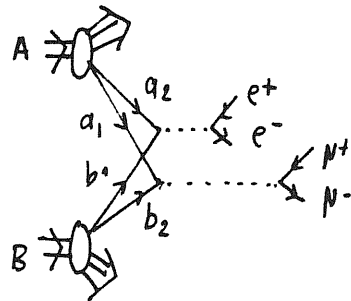


Fig. 2B: The double Drell-Yan process under investigation, with two different pairs (e^+e^-) and ($\mu^+\mu^-$)

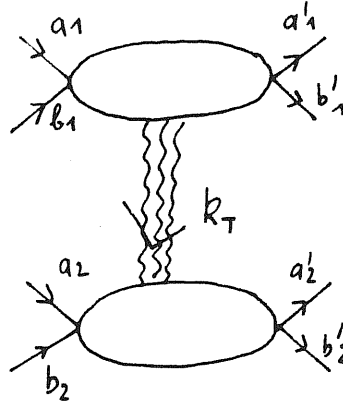


Fig. 3B: The boundedness of $k_T = \sum_i k_{Ti} \sim \frac{1}{R}$

b) The double Drell-Yan cross section formula

We generalize to the double Drell-Yan the formula which relates the differential cross section $\frac{d\sigma}{dQ^2}$ to $\hat{\sigma}$, where $\hat{\sigma}$ is the total cross section for partons to annihilate into a massive photon of mass Q . For the double Drell-Yan and for the case of two distinct lepton pairs e.g. $(e^+e^-, \mu^+\mu^-)$ we get the simple generalization

$$\frac{d\sigma}{dQ_1^2 dQ_2^2} = \left(\frac{\alpha}{3\pi}\right)^2 \frac{1}{Q_1^2 Q_2^2} \int dx_1 dx_2 dy_1 dy_2 d\frac{\Delta}{T} G_A^+(x_1, x_2, \frac{\Delta}{T}) \tilde{\sigma} G_B^-(y_1, y_2, \frac{\Delta}{T}). \quad (3.\tilde{B})$$

In Eq. (3.B) $\tilde{\sigma}$ is the disconnected (up to radiative correction) cross section to produce two massive photons of mass Q_1 and Q_2 . The factor $\left(\frac{\alpha}{3\pi}\right)^2 \frac{1}{Q_1^2 Q_2^2}$ comes from integrations over the angular distribution of the double lepton pairs.

From now on we concentrate on the hard cross section $\tilde{\sigma}$ in formula (3.B). We have said that the cross sections $\tilde{\sigma}_{\alpha\alpha'}$ are linear combinations of well-defined elementary cross sections σ_{KL}^{IJ} . Does one include connecting gluons in computing these cross sections? At (LLA) and to any order in α_s , e.g. $(\alpha_s)^n$ non-connecting gluons contribute a logarithmic term of the form $(\alpha_s \ln Q_i^2)^n$, while at

the same order connecting gluons contribute just a finite term at high Q ; owing to the boundedness of $k_T = \sum_i k_{Ti}$, in fact we have the result

$$\int_1^Q \frac{d^2 k_{T1}}{k_{T1}^2} \frac{d^2 k_{T2}}{k_{T2}^2} \dots \frac{d^2 k_{Tn}}{k_{Tn}^2} \theta(\langle P_T^2 \rangle - (k_{T1} + k_{T2} + \dots + k_{Tn})^2) \underset{Q^2 \rightarrow \infty}{\sim} c t_e \quad (4.\tilde{B}a)$$

where $\langle P_T^2 \rangle$ is the mean value of the squared intrinsic transverse momentum of the partons, $Q \sim Q_i (i=1,2)$ and λ is a gluonic infrared regularization mass.

Eq. (4. $\tilde{B}a$) can be seen rather easily in the case of one or two gluons insertions, for example. In the one gluon case we have the integral

$$\int_1^Q \frac{d^2 k_{T1}}{k_{T1}^2} \theta(\langle P_T^2 \rangle - k_{T1}^2) \sim \int \frac{d^2 k_{T1}}{k_{T1}^2} \sim \ln \langle P_T^2 \rangle \quad (4.\tilde{B}b)$$

For the two gluons one has to compute the following integral

$$\int_1^Q \frac{d^2 k_{T1}}{k_{T1}^2} \frac{d^2 k_{T2}}{k_{T2}^2} \theta(\langle P_T^2 \rangle - (k_{T1} + k_{T2})^2) \quad (4.\tilde{B}c)$$

For fixed k_{T2} , the momentum k_{T1} spans the whole circle shown in Fig. 4 \tilde{B} .

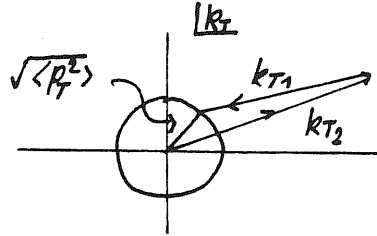


Fig. 4 \tilde{B} : Domain of integration

For large Q one can put $k_{T1} \sim k_{T2}$ and therefore the integral reads

$$\int^Q \frac{d^2 k_{T2}}{(k_{T2}^2)^2} \int^{\langle P_T^2 \rangle} d^2 k_{T1} \sim \frac{\langle P_T^2 \rangle}{Q^2} . \quad (4.\tilde{B}d)$$

Therefore owing to the result (4. $\tilde{B}a$) connecting gluons are not leading with respect to non-connecting ones and so one simply ignores them. Thus the double Drell-Yan process which is disconnected at the parton level (zeroth order in α_s) remains disconnected to any leading order in α_s .

At first sight, one might think that there is no simple relation between the elementary cross section defined above σ_{KL}^{IJ} . This however is not true in processes where connecting gluons are not present as it is in the case for the double Drell-Yan under study. In fact we have the following relationships

$$\sigma_{KL}^{(0)IJ} = W_{KL}^{(0)IJ} \sigma_{DD}^{(0)} \quad (5.\tilde{B})$$

where $W_{KL}^{(0)IJ}$ are simple numerical constants, and the cross sections are computed at the zeroth order in α_s . $W^{(0)}$ has the simple form

$$W^{(0)} = \begin{pmatrix} 1 & \frac{1}{N} & \frac{1}{2} & \frac{1}{2N} \\ \frac{1}{N} & 1 & \frac{1}{2N} & \frac{1}{2} \\ \frac{1}{2} & \frac{1}{2N} & \frac{1}{2} & \frac{1}{2N} \\ \frac{1}{2N} & \frac{1}{2} & \frac{1}{2N} & \frac{1}{2} \end{pmatrix} \quad (6.\tilde{B})$$

To work out $W^{(0)}$, one computes the components σ_{KL}^{IJ} . They involve the following traces

$$\begin{aligned}
\sigma_{DD}^{(0)IJ} &\simeq C^{IJ} T_2 \gamma_\nu p_A^\nu \gamma^\mu p_B^\mu \cdot T_2 \gamma_\nu p_A^\nu \gamma^\mu p_B^\mu \cdot \\
\sigma_{EE}^{(0)IJ} &\simeq C^{IJ} T_2 \gamma_\nu p_A^\nu \gamma^\mu p_B^\mu \cdot T_2 \gamma_\nu p_A^\nu \gamma^\mu p_B^\mu \cdot \\
\sigma_{ED}^{(0)IJ} &\simeq C^{IJ} T_2 \gamma_\nu p_A^\nu \gamma^\mu p_B^\mu \gamma_\nu p_A^\nu \gamma^\mu p_B^\mu \cdot
\end{aligned} \tag{7. \tilde{B}}$$

where the coefficients C^{IJ} have the values

$$\begin{aligned}
C^{EE} &= C^{DD} = N^2 \\
C^{ED} &= C^{DE} = N
\end{aligned} \tag{8. \tilde{B}}$$

The above traces are easy to compute and give the following relations

$$\sigma_{DE}^{(0)IJ} = \sigma_{ED}^{(0)IJ} = \sigma_{EE}^{(0)IJ} = \frac{\sigma_{DD}^{(0)IJ}}{2} \quad I, J = D, E \tag{9. \tilde{B}}$$

$$\sigma_{KL}^{(0)DE} = \sigma_{KL}^{(0)ED} = \frac{\sigma_{KL}^{(0)DD}}{N} \tag{10. \tilde{B}}$$

$$\sigma_{KL}^{(0)EE} = \sigma_{KL}^{(0)DD} \quad K, L = D, E \tag{11. \tilde{B}}$$

Now does the above relationship remain valid to any order in α_s ?

This is true for all the components σ_{kl}^{IJ} except for the particular colour projection σ_{KL}^{EE} . Eq. (9. \tilde{B}) referring to the spin are true at (LLA) to any order in α_s due to the helicity conservation. For Eq. (10. \tilde{B}) their generalization to any order may be seen by direct calculations of the colour factors of the cross sections σ_{kl}^{IJ} . Another method consists in replacing each gluon line by an oriented colour anti-gluon line⁽⁴³⁾ and counting the number of the resulting colour loops.

The component σ_{KL}^{EE} needs more care, in fact inspection of Fig. 2A.b shows that its colour structure does not allow the emission of one real gluon only (Fig. 5B)



Fig. 5B: a) This real gluon is forbidden by the colour structure
b) The corresponding virtual gluon is no longer compensated

Therefore the virtual non-connecting gluon is no longer compensated as is the case for single Drell-yan or deep inelastic scattering. Hence at (LLA) and to order α_s , σ_{KL}^{EE} has the form

$$\sigma_{KL}^{(1)EE} = \left(1 - \frac{2\alpha_s}{3\pi} \ln^2\left(\frac{Q_1^2}{\lambda^2}\right) - \frac{2\alpha_s}{3\pi} \ln^2\left(\frac{Q_2^2}{\lambda^2}\right) + \dots\right) \sigma_{KL}^{(0)EE} \quad (12.\tilde{B})$$

Now at second and higher order only the singlet part of the virtual gluonic non-connecting system is compensated by the corresponding part in the real non-connecting system. To see it define

$$\sigma^{EE}(n) = \sum_{r=0}^{\infty} \sigma^{EE}(n, r) \quad (\text{we omit the indices K, L}) \quad (13.\tilde{B})$$

where $\sigma^{EE}(n, r)$ is the contribution to the cross section of the diagrams with n real gluons and r virtual gluons. We have the following relations

$$\begin{aligned} \sigma^{DD}(0) &\simeq \frac{\sigma^{DD}(1)}{Q^2 \rightarrow \infty} \simeq 0 \quad (\text{Sudakov suppression}) \\ \sigma^{EE}(0) &= \sigma^{DD}(0) \\ \sigma^{EE}(1) &= 0 \\ \sigma^{EE}(n) &= \frac{\sigma^{DD}(n)}{N^2} \quad n \geq 2. \end{aligned} \quad (14.\tilde{B})$$

Therefore the cross section σ^{EE} to all orders is given by

$$\sigma^{EE} = \sum_{n=0}^{\infty} \sigma_{(n)}^{EE} \frac{1}{Q^2} = \sum_{n=0}^{\infty} \frac{\sigma^{DD(n)}}{N^2} = \frac{\sigma^{DD}}{N^2} \quad (15. \tilde{B})$$

So at very large Q^2 we have the relation

$$\sigma^{EE} = \frac{\sigma^{DD}}{N^2} \quad (Q^2 \gg 1) \quad \text{and all radiative corrections (16. } \tilde{B}) \text{ to any order are summed up}$$

As a consequence the component W_{KL}^{EE} takes on the value 1 when only the Born contribution is taken into account (case a) or the value $\frac{1}{N^2}$ at very high Q^2 and when one includes all radiative corrections (case b) in which case W takes on the following form

$$W = \begin{pmatrix} 1 & \frac{1}{N} & \frac{1}{2} & \frac{1}{2N} \\ \frac{1}{N} & \frac{1}{N^2} & \frac{1}{2N} & \frac{1}{2N^2} \\ \frac{1}{2} & \frac{1}{2N} & \frac{1}{2} & \frac{1}{2N} \\ \frac{1}{2N} & \frac{1}{2N^2} & \frac{1}{2N} & \frac{1}{2N^2} \end{pmatrix} \quad (17. \tilde{B})$$

Thus we succeed in writing for the double Drell-Yan, all the colour and spin projections σ_{KL}^{IJ} in terms of only one i.e. σ_{DD}^{DD} . Moreover since connecting gluons are neglected σ_{DD}^{DD} factorizes as

$$\sigma_{DD}^{DD} = \sigma_1 \sigma_2 \quad (18. \tilde{B})$$

where σ_1 and σ_2 are two uncorrelated single Drell-Yan cross sections which are computed to all orders in α_s in the usual way.

To compute the hadronic cross sections in Eq. (3. \tilde{B}) we come back to

$\tilde{\sigma}_{\alpha\alpha'}^{ii'}$ which are linear combinations of σ_{KL}^{IJ} whose coefficients are fixed by the Π expansions Eq. (21. \tilde{A}) and Eq. (28. \tilde{A}). Using the matrix $W^{(0)}$ or W we can write $\tilde{\sigma}_{\alpha\alpha'}^{ii'}$ in terms of $\sigma_1 \sigma_2$ only and we find that $\tilde{\sigma}_{\alpha\alpha'}^{ii'}$ is diagonal. In the physical basis we have

chosen for the expansion of the cut amplitude $\tilde{\Gamma}$

$$\tilde{\sigma}_{\alpha\alpha'}^{ii'} = A_i \delta_{ii'} \delta_{\alpha\alpha'} \sigma_1 \sigma_2 \quad (\text{no summation over } i) \quad (19.\tilde{B})$$

with $A_1 = \frac{4N}{N-1}$ (case a, Born approximation)

$$A_2 = \frac{4N}{N+1}$$

and $A_1 = A_2 = 2$ (case b, $Q^2 \gg 1$ and all radiative corrections to any order are summed up)

Going back to formula (3. \tilde{B}) the cross section for the double Drell-Yan takes on the final and very simple form

$$\frac{d\sigma}{dQ_1^2 dQ_2^2} = \left(\frac{\alpha}{3\pi}\right)^2 \frac{1}{Q_1^2 Q_2^2} \int dx_1 dx_2 dY_1 dY_2 d\hat{Q}_T^2 [A_1 (G_{A1}' G_{B1}' + G_{A2}' G_{B2}' + G_{A3}' G_{B3}') + A_2 (G_{A1}^2 G_{B1}^2 + G_{A2}^2 G_{B2}^2 + G_{A3}^2 G_{B3}^2)] \sigma_1 \sigma_2 \quad (20.B)$$

\tilde{C}) The evolution equation of the structure functions

The structure functions G_b^c defined in the previous sections evolve in a non-trivial way in the sense that radiative corrections mix between them. In the present section we propose to study this evolution in the approximation that all exchanged terms are neglected. Therefore only the direct term will be considered and it is described by the component σ_{00}^{00} . This approximation amounts to considering just the diagram (2 \tilde{A} .a) which corresponds to two uncorrelated Drell-Yan cross sections. At order α_s , the gluon distributions are also participating in the evolution of the quark distributions. We shall neglect their contributions in the following analysis, therefore the evolution equation we shall get should be taken as an approximation. The double Drell-Yan cross section in the Born approximation reads

$$\frac{d\sigma}{dQ_1^2 dQ_2^2} = \left(\frac{4}{9} \pi \alpha^2\right)^2 \frac{e_q^4}{s^2 Q_1^2 Q_2^2} \int \frac{dx_1}{x_1} \frac{dx_2}{x_2} \frac{dy_1}{y_1} \frac{dy_2}{y_2} \frac{d\Delta_T^2}{T} G_A G_B \delta(1-\hat{\tau}_1) \delta(1-\hat{\tau}_2). \quad (1.\tilde{C})$$

Where $\hat{\tau}_i = \frac{Q_i^2}{\hat{s}_i}$ and G_A, G_B are the double structure functions summed over spin and colour quantum numbers.

At the one gluon level where the gluon is inserted in all possible ways, the cross section has the form

$$\begin{aligned} \frac{d\sigma}{dQ_1^2 dQ_2^2} = & \left(\frac{4}{9} \pi \alpha^2\right)^2 \frac{e_q^4}{s^2 Q_1^2 Q_2^2} \int [\delta(1-\hat{\tau}_1) \delta(1-\hat{\tau}_2) + \frac{2\alpha_s}{2n} P(\hat{\tau}_1) \tilde{t}_1 \delta(1-\hat{\tau}_2) + \frac{2\alpha_s}{2n} P(\hat{\tau}_2) \tilde{t}_2 \delta(1-\hat{\tau}_1)] \\ & \times G_A(x_1, x_2, \Delta_T) G_B(y_1, y_2, \Delta_T) \frac{dx_1}{x_1} \frac{dx_2}{x_2} \frac{dy_1}{y_1} \frac{dy_2}{y_2} \frac{d\Delta_T^2}{T}. \end{aligned} \quad (2.\tilde{C})$$

where $P(\hat{\tau}_i)$ is the Altarelli-Parisi probability

$$P(\hat{\tau}_i) = \frac{4}{3} \left[\frac{1+\hat{\tau}_i^2}{(1-\hat{\tau}_i)_+} + \frac{3}{2} \delta(1-\hat{\tau}_i) \right]. \quad (3.\tilde{C})$$

$$\text{and } \tilde{t}_i = \ln \frac{Q_i^2}{\lambda^2}.$$

In analogy with the single Drell-Yan case we proceed by "renormalizing" the mass singularities, therefore

$$\begin{aligned} \frac{d\sigma}{dQ_1^2 dQ_2^2} = & \left(\frac{4}{9} \pi \alpha^2\right)^2 \frac{e_q^4}{s^2 Q_1^2 Q_2^2} \int [\delta(1-\hat{\tau}_1) \delta(1-\hat{\tau}_2) + \frac{2\alpha_s}{2n} P(\hat{\tau}_1) \tilde{t}_1 \delta(1-\hat{\tau}_2) + \frac{2\alpha_s}{2n} P(\hat{\tau}_2) \tilde{t}_2 \delta(1-\hat{\tau}_1)] \\ & \times G_A G_B \frac{dx_1}{x_1} \frac{dx_2}{x_2} \frac{dy_1}{y_1} \frac{dy_2}{y_2} \frac{d\Delta_T^2}{T}. \end{aligned} \quad (4.\tilde{C})$$

where now $\tilde{t}_i = \ln \frac{Q_i^2}{Q_0^2}$, here $G_A \equiv G_A(x_1, x_2, \Delta_T, Q_0^2, \lambda)$ is finite in the limit $\lambda \rightarrow 0$ and Q_0 is a mass introduced by writing as usual.

$$1 + \alpha_s \ln \frac{Q^2}{\lambda^2} + \dots = (1 + \alpha_s \ln \frac{Q^2}{Q_0^2} + \dots) (1 + \alpha_s \ln \frac{Q_0^2}{\lambda^2} + \dots) \quad (5.\tilde{C})$$

The Q^2 independence of the second multiplicative factor allows its

absorption into G^{1s} . The equation for $\frac{d\sigma}{dQ_1^2 dQ_2^2}$, Eq. 4C can formally be rewritten as

$$\frac{d\sigma}{dQ_1^2 dQ_2^2} = \left(\frac{4}{9} \pi \alpha^2\right)^2 \frac{e_q^4}{s^2 Q_1^2 Q_2^2} \int_0^1 \prod_{i=1}^2 \frac{dx_i}{x_i} \frac{dy_i}{y_i} d\hat{\Lambda}_7^2 G_A(x_1, x_2, t_1, t_2, \frac{\hat{\Lambda}_7}{7}) \times G_B(y_1, y_2, t_1, t_2, \frac{\hat{\Lambda}_7}{7}) \delta(1-\hat{\tau}_1) \delta(1-\hat{\tau}_2). \quad (6.\tilde{C})$$

We can do this if G_A obeys the following differential equation

$$\begin{aligned} \frac{\partial G_A(x_1, x_2, t_1, t_2)}{\partial t_1} &= \frac{\alpha_s}{2\pi} \int_{x_1}^{1-x_2} \frac{dy}{y} P\left(\frac{x_1}{y}\right) G_A(y, x_2, t_1, t_2) \\ \frac{\partial G_A(x_1, x_2, t_1, t_2)}{\partial t_2} &= \frac{\alpha_s}{2\pi} \int_{x_2}^{1-x_1} \frac{dy}{y} P\left(\frac{x_2}{y}\right) G_A(x_1, y, t_1, t_2). \end{aligned} \quad (7.\tilde{C})$$

and similarly for G_B . Phenomenologically one is interested in the small x region so one can forget about the x -dependence of the upper bound of the integrations in Eq.(7.C).

This system of first order differential equations is simply rewritten in terms of double moments $M_{np}(t_1, t_2)$. We define them as

$$M_{np}(t_1, t_2) = \int_0^1 dx_1 \int_0^{1-x_1} dx_2 x_1^{n-1} x_2^{p-1} G_A(x_1, x_2, t_1, t_2) \quad (8.\tilde{C})$$

The system is relatively simple in terms of these moments

$$\begin{aligned} \frac{\partial M_{np}(t_1, t_2)}{\partial t_1} &= \frac{\alpha_s}{2\pi} A_n M_{np}(t_1, t_2) \\ \frac{\partial M_{np}(t_1, t_2)}{\partial t_2} &= \frac{\alpha_s}{2\pi} A_p M_{np}(t_1, t_2) \end{aligned} \quad (9.\tilde{C})$$

With $A_n = \int_0^1 z^{n-1} p(z) dz$ and $A_p = \int_0^1 z^{p-1} p(z) dz$ (10.~C)

The solution of it is straightforward.

$$M_{np}(t_1, t_2) = M_{np}(0, 0) \left[1 + \frac{\alpha_s}{2n} (A_n t_1 + A_p t_2) + \dots \right] \quad (11.~\tilde{C})$$

We have defined the moment of $G_A(x_1, x_2, Q_1, Q_2)$ which depends on two large masses Q_1 and Q_2 . We concentrate on the case where Q_1 and Q_2 are of the same order of magnitude. In this case the moment is a function of a unique large scale Q ($Q^2 = Q_1 Q_2$) and a parameter η ; $\eta = \frac{Q_2^2}{Q_1}$ which can eventually be kept fixed.

Define $t = \frac{t_1 + t_2}{2} = \ln \frac{Q^2}{Q_0^2}$
 $\tau = \frac{t_1 - t_2}{2} = \ln \eta$ (12.~C)

then

$$M_{np}(t_1, t_2) = M_{np}(Q^2, \eta) = M_{np}(Q_0^2) \left[1 + \frac{\alpha_s}{2n} (A_n + A_p) \ln \frac{Q^2}{Q_0^2} + \dots \right. \\ \left. + \frac{\alpha_s}{2n} (A_n - A_p) \ln \eta + \dots \right] \quad (13.~\tilde{C})$$

First order corrections at (LLA) are of the form

$$\alpha_s(\mu^2) \ln Q^2 \quad (14.~\tilde{C})$$

In order that the correction of the order $(\alpha_s)^n$ be negligible, it is natural to choose the renormalization point as

$$\mu^2 = Q^2 \quad (15.~\tilde{C})$$

In this case $\alpha_s(Q^2) \ln Q^2$ is of order unity and to be consistent, one has to sum up all terms of the form

$$(\alpha_s(Q^2) \ln Q^2)^n \quad (16.\tilde{C})$$

This is done usually by using the renormalization group equation. One finds that

$$M_{np} = q_{np} [\alpha_s(Q^2)]^{-\frac{A_{np}}{2\pi b}} \quad (17.\tilde{C})$$

where q_{np} is the presently uncalculable non-perturbative part and A_{np} is related to the anomalous dimension which is unknown. The coefficient b is given as usual by

$$b = \frac{33 - 2N_f}{12\pi} \quad N_f = \text{number of flavour} \quad (18.\tilde{C})$$

Expanding M_{np} one obtains

$$M_{np}(Q^2) = M_{np}(Q_0^2) \left[1 + \frac{\alpha_s(Q^2)}{2\pi} A_{np} \ln \frac{Q^2}{Q_0^2} + \dots \right] \quad (19.\tilde{C})$$

The unknown coefficient is then given by identification with the first order calculation Eq. (11. \tilde{C})

$$A_{np} = A_n + A_p \quad (20.\tilde{C})$$

The result of Eq. (17. \tilde{C}) is the solution of the differential equation

$$\frac{\partial M_{np}(t, \tau)}{\partial t} = \frac{\alpha_s(t)}{2\pi} A_{np} M_{np}(t, \tau) \quad (21.\tilde{C})$$

Going back to the structure function $G_A(x_1, x_2, t, \tau)$ one obtains the evolution equation for the double structure function which reads

$$\begin{aligned} \frac{\partial G_A(x_1, x_2, t, \tau, \frac{\Delta}{\tau})}{\partial t} = & \frac{\alpha_s(t)}{2\pi} \int_{x_1}^{1-x_2} \frac{dy}{y} P\left(\frac{x_1}{y}\right) G_A(y, x_2, t, \tau, \frac{\Delta}{\tau}) \\ & + \frac{\alpha_s(t)}{2\pi} \int_{x_2}^{1-x_1} \frac{dy}{y} P\left(\frac{x_2}{y}\right) G_A(x_1, y, t, \tau, \frac{\Delta}{\tau}) . \end{aligned} \quad (22.\tilde{C})$$

A similar equation is obtained for $G_B(y_1, y_2, t, \tau, \frac{\Delta}{\tau})$.

IV CONCLUSIONS

In this thesis we have discussed hard disconnected multiparton processes. We showed that they may play a central role in the description of a large class of reactions such as, wide angle elastic scattering, single particle inclusive reactions, multijet production and $w +$ multijet production.

Multiparton processes are power corrections to the leading process (single scattering). It is however particularly important to note that

- The suppression factor, in the kinematical region $E_T \ll S$, is not $\frac{1}{R^2 S}$ as it might appear at first sight but rather $\frac{1}{R^2 E_T^2}$.
- Due to the steepness of the parton cross sections, it may become more economical at fixed E_T to have several parton scatterings, each at relatively low P_T , rather than a single one with large P_T . The multiparton mechanism is also interesting in that it provides a probe of the parton correlations in x (longitudinal momentum fraction), in Δ_T (relative transverse distance), in spin and in colour. A number of theoretical problems have been already clarified, in particular the correct introduction by N. Paver and D. Treleani of the transverse degree of freedom (Δ_T) in the double structure function. For our part we have analysed the double Drell-Yan mechanism as the simplest example of multiparton scattering. Particular attention has been given to the spin and colour structure as well as to the factorizability of the process. We have shown that connecting gluons which apparently lead to violation of factorization, in fact have no influence at the leading log approximation. We worked out the double Drell-Yan cross section by taking explicitly the quark spin and colour degrees of freedom. These led us to introduce six newly defined structure functions $G_b^c(x_1, x_2, \Delta_T)$ generalizing the familiar ones and showed that these are convoluted with two completely uncorrelated single Drell-Yan cross sections.

The method we have developed in this thesis to deal with the double Drell-Yan cross section is generalizable, in principle, to any multiparton scattering. Many other problems remain to be investigated, a particularly interesting one is the analysis of the evolution of the multiparton distribution functions G_b^c , which is not a trivial matter due to their mixing under radiative corrections.

V) APPENDIX

We first consider the contribution of "non-connecting" gluons to the diagrams of Fig. 3Aa. This amounts to correcting the quark-quark or the quark-antiquark scattering depicted in Fig. I

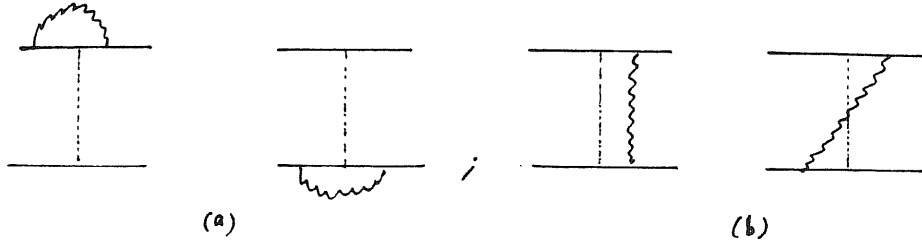


Fig. I: First order correction to quark-quark or quark-antiquark scattering (wavy lines are soft gluons)

The gluons in Fig. I are soft in the sense that one may neglect in the numerator their momentum k compared with an external P (provided that one is interested only in the leading log contribution).

The calculation of the integrations in Fig. I is exactly similar to that of the quark form factor. In fact one can ignore the hard gluon propagator in the case of Fig. Ib provided that t is of the same order of S , because it already carries momentum transfer of order t and so the addition of the soft gluon momentum to it is negligible in comparison. therefore we only sketch the vertex correction calculations using a phase space technique to work out directly the leading log terms. This technique has the advantage of being suitable to higher order corrections.

a) The one gluon insertion

We calculate the leading contribution to the quark/photon vertex Fig. II

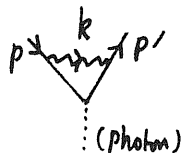


Fig. II: First order QCD contribution to the quark form factor

Both external quark lines are taken to be off shell i.e. $\Delta = p^2 - m^2 \neq 0$
 $\Delta' = p'^2 - m^2 \neq 0$ and we put $T = 2p \cdot p'$.

The gluon being soft in the sense discussed above, the dominant term requires no cut-off in the integral, and the numerator is just $2T$ times the bare quark/photon vertex. The colour factor is C_F . Hence the net effect asymptotically is to multiply the bare quark/photon vertex by

$$2T C_F i \frac{g^2}{(2\pi)^4} \int \frac{d^4 k}{(k^2 + i\varepsilon) [(k-p)^2 - m^2 + i\varepsilon] [(k-p')^2 - m^2 + i\varepsilon]} \quad (1)$$

We evaluate the asymptotic behaviour of the integral by writing

$$k = x p + y p' + k_T.$$

where k_T is transverse to both p and p' . We then use x, y and k_T as integration variables instead of k . We have

$$\begin{aligned} k^2 &= xyT + x^2 p^2 + y^2 p'^2 - k_T^2 \sim xyT - \vec{k}_T^2 \\ (k-p)^2 &= (x-1) yT + (x-1)^2 p^2 + y^2 p'^2 - \vec{k}_T^2 \sim -yT + p^2 - \vec{k}_T^2 \\ (k-p')^2 &= x(y-1)T + x^2 p^2 + (y-1)^2 p'^2 - \vec{k}_T^2 \sim xT + p'^2 - \vec{k}_T^2 \end{aligned} \quad (2)$$

We note that all three denominator factors in (1) are smallest when both x and y are small, so that the region of small x and y gives the dominant contribution to the integral. This justifies the approximation in (2) and gives

$$C_F T / (2\pi)^4 i \frac{g^2}{(2\pi)^4} \int dx dy d^2 k_T \frac{1}{(xyT - k_T^2 + i\varepsilon)(-yT - k_T^2 + D + i\varepsilon)(xT - k_T^2 + D' + i\varepsilon)} \quad (3)$$

This x integration vanishes because of the $i\epsilon$ unless $y > 0$. It gives

$$C_F \frac{g^2}{8\pi^2} \int_0^\infty dy dk_T^2 \frac{1}{(-y\tau - k_T^2 + \Delta + i\epsilon) [-k_T^2(1+y) + y\Delta' + i\epsilon]} \quad (4)$$

Now instead of doing the y integration which is the simplest way to do it, we use instead a phase space method which is most readily applicable to the study of two-gluon insertions. We write

$$\begin{aligned} y &= |\tau|^{-\alpha} \\ k_T^2 &= |\tau|^\lambda \end{aligned} \quad (5)$$

so that
$$\int_0^\infty dy dk_T^2 = \int_{-\infty}^\infty |\tau|^{1-\alpha} \ln^2 |\tau| d\lambda d\alpha \quad (6)$$

The dominant contribution to the integrations comes from values of λ and α such that the denominator cancels the variable power of $|\tau|$ in (6). This is so that doing the integrations does not again remove the $\ln^2 |\tau|$ factor. To achieve this, $(-y\tau)$ must dominate over the other terms in the first factor of the denominator, and $(-k_T^2)$ must dominate in the second factor. This determines the dominant part of the integration region to be

$$\begin{aligned} 1 > \alpha > 0 \\ 1 - \alpha > \lambda > -\alpha \end{aligned} \quad (7)$$

This region has a unit volume (see Fig III)

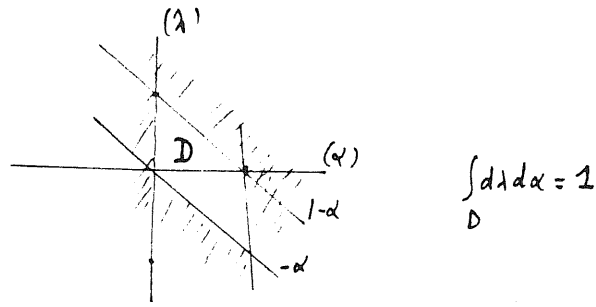


Fig.III: Dominant phase space

So we have the final result $-C_F F(r)$, where

$$F(r) = \frac{g^4}{8\pi^2} \ln^2 |r|. \quad (8)$$

b) The two gluon insertion

Now we are interested in diagrams that give a \ln^4 contribution. These are given by Fig.IV

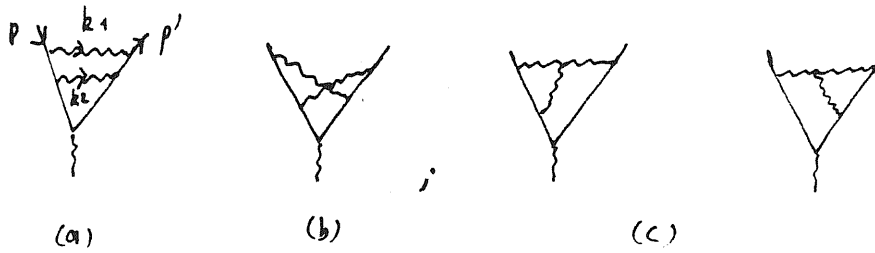


Fig. IV: Second-order correction to the quark form factor

In the case of Fig. IVa, the bare vertex is multiplied by

$$-C_F \frac{g^4}{(2\pi)^8} \int dx_1 dy_1 d\vec{k}_{T1} dx_2 dy_2 d\vec{k}_{T2} \frac{1}{(x_1 y_1 \tau - k_{T1}^2 + i\epsilon)(-y_1 \tau - k_{T1}^2 + D + i\epsilon)(-x_2 \tau - k_{T2}^2 + D' + i\epsilon)} \times [-(y_1 + y_2) \tau - (\vec{k}_{T1} + \vec{k}_{T2})^2 + D + i\epsilon] [-(x_1 + x_2) \tau - (\vec{k}_{T1} + \vec{k}_{T2})^2 + D' + i\epsilon]. \quad (9)$$

The x_1 and x_2 integration can be done by counter manipulations, given

$$C^2 T^2 \left(\frac{q^2}{8\pi^2} \right)^2 \int_0^\infty \frac{dy_1}{y_1} \frac{dy_2}{y_2} \frac{dk_{1T}}{\pi} \frac{dk_{2T}}{\pi} \frac{1}{(-y_1^2 - k_{1T}^2 + \Delta) [-(y_1 + y_2)^2 - (\vec{k}_{1T} + \vec{k}_{2T})^2 + \Delta]} \times \left(-\frac{k_{1T}^2}{y_1} - k_{1T}^2 + \Delta' \right) \left[-\frac{k_{1T}^2}{y_1} - \frac{k_{2T}^2}{y_2} - (\vec{k}_{1T} + \vec{k}_{2T})^2 + \Delta' \right]. \quad (10)$$

We next change variables as in (5) and obtain inequalities analogous to (7) that produce cancellation of the variable power of $|\vec{r}|$ coming from the Jacobian (see 6) i.e.

$$\begin{aligned} 1) & \alpha_1 > \alpha_2 > 0 \\ 1) & \alpha_2 + \lambda_2 > \lambda_1 + \alpha_1 > 0 \end{aligned} \quad (11)$$

The volume of the integration region (11) is $\frac{1}{4}$ (see Fig. V), so we have the result

$$\frac{1}{4} C_F^2 (F(\tau))^2$$

$F(\tau)$ is again given by (8)

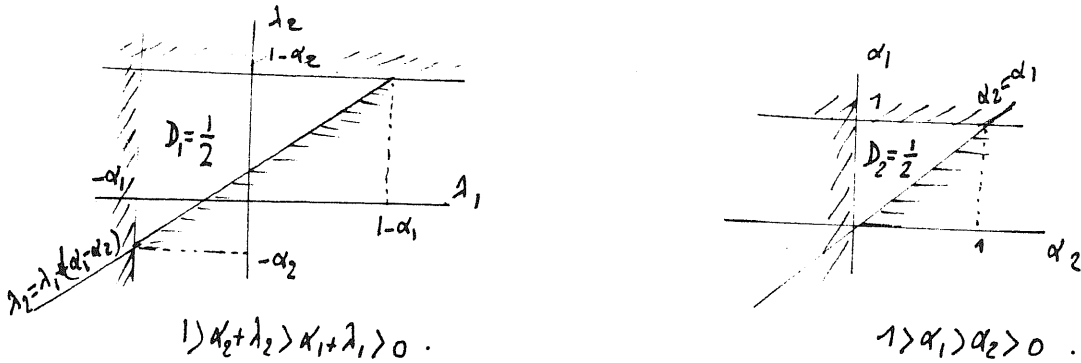


Fig. V: Dominant phase space for the diagram IVa.

One can go along the same lines for the diagrams of Fig. IVb,c. Other diagrams to consider are those depicted in Fig. VI

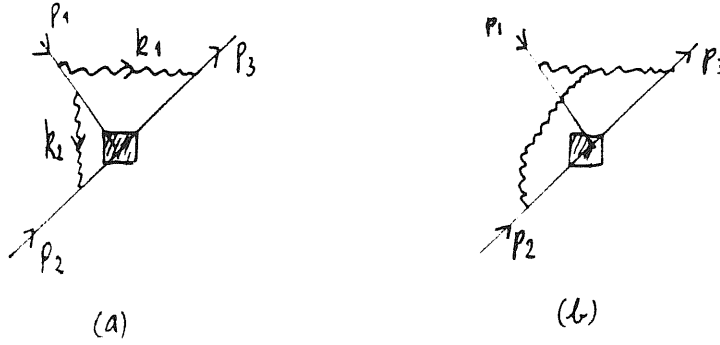


Fig. VI: Soft gluon insertions, with hard interactions denoted by the square blobs. All three external invariants are large

It turns out that in the fixed angle limit the type of insertion shown in Fig. VIb does not yield a \log^4 factor, but Fig. VIa does.

To deal with the multiple scattering diagram, one has to insert "connecting" gluons as well. The calculation of their contributions is similar to that for the "non-connecting" gluons with the important difference that k_T is bounded, and this reduces the corresponding phase space volume. Summing the contributions of all diagrams one gets the factors necessary to build up the exponential factor.

REFERENCES

- (1) P.V. Landshoff, Phys. Rev. D10, 1024 (1974).
- (2) P.V. Landshoff and D.J. Pritchard, Z Physik C Particle and Fields 6, 69 (1980).
- (3) H.D. Politzer, Nucl. Phys. B172 (1980) 349.
- (4) R.K. Ellis, W. Furmanski, R. Petronzio, Nucl. Phys. B207 (1982) 1.
- (5) S-J. Brodsky and G.R. Farrar; Phys. Rev. Lett. 31, 1153 (1973);
V.A. Matveev et al.: Lett. Nuovo Cimento 7, 719 (1973);
S-J Brodsky and G.R. Farrar, Phys. Rev. D11, 1309 (1975).
- (6) M. Jacob, CERN Preprint TH-3693 (1983), TH-3728 (1983).
- (7) N. Paver and D. Trealeani, Nuovo Cimento 70A (1982) 215;
Nuovo Cimento 73A (1983) 392, Preprint SISSA 60/83/EP to appear in
Phys. Lett; Preprint SISSA 43/84/EP (1984). To appear in Z Phys. C.P./Fields
- (8) B. Humpert, Phys. Lett. 131B (1983) 461, CERN Preprint TH-3720
(1983); B. Humpert and R. Odorico, Lecture presented at the
4th Topical Workshop on proton-antiproton collider physics,
Bern, March 5-8, 1984.
- (9) M.Mekhfi, SISSA preprint 46.83.EP (1983, to appear in Nucl.
Phys. B.
- (10) R. Blankenbecler, S.J. Brodsky, and J.F. Gunion, Phys. Lett.
39B, 649 (1972); Phys. Rev. D8, 187 (1973).
- (11) D. Horn and M. Moshe, Nucl. Phys. B48, 557 (1972).
- (12) D. Cline, F. Halzen and M. Waldrop, Nucl. Phys. B55, 157 (1973).
- (13) A. Donnachie, P.V. Landshoff: Z. Phys. C2, 55 and 372 (1979).
- (14) S.J. Brodsky, G.P. Lepage; SLAC-PUB-2294.
- (15) A. Duncan, A.H. Mueller, Phys. Lett. 90B, 159 (1980).
- (16) J.M. Cornwall, G. Tiktopoulos, Phys. Rev. D13, 3370 (1976);
E.C. Poggio, H.R. Quinn, Phys. Rev. D12, 3279 (1975).
- (17) G. Parisi, Phys. Lett. 84B, 225 (1979).
- (18) B. Alper et al., Nucl. Phys. B89, 19 (1975).

- (19) See the reviews by P.V. Landshoff and S.D. Ellis, in Proceedings of the XVII International Conference on High Energy Physics, London (1974), edited by J.R. Smith (Rutherford Laboratory, Chilton, Didcot, Berkshire, England 1974) and also lectures by R. Blankenbecler and S. Brodsky, SLAC summer institute on particle physics, SLAC Report No. SLAC-179, 1974 (unpublished).
- (20) X. Artru and M. Mekhfi, Phys. Rev. D22, 751 (1980).
- (21) C.T. Sachrajda, Phys. Lett. 76B (1978), 100.
- (22) W. Furmanski, Phys. Lett. 77B (1978), 312.
- (23) P.V. Landshoff, J.C. Pokkinghorne and D.M. Scott, Phys. Rev. D12, 3738 (1975).
- (24) UA2 Coll. P. Bagnaria et al. Z. Phys. C 20 (1983) 117;
UA1 Coll. G. Arnison et al. Phys. Lett. 123B (1983), 115.
- (25) UA2 Coll. M. Banner et al., Phys. Lett; 118B (1982), 203;
UA1 Coll. A. Arnison et al., Phys. Lett. 132B (1983), 214.
- (26) Tasso Coll. R. Brandelik et al., Phys. Lett. 86B (1979), 243;
Pluto Coll. C.H. Berger et al., Phys. Lett. 86B (1979), 418;
Mark-J Coll. D.P. Barber et al., Phys. Rev. Lett. 43 (1979) 830.
- (27) Z. Kunszt and E. Pietarinen, Phys. Lett. 132B (1983), 453;
R. Odorico: CERN Preprint TH-3744 (1983) and references therein.
- (28) P.V. Landshoff and J. Polkinghorne, Phys. Rev. D18 (1978) 3344.
- (29) A. Bassetto, B. Ciafaloni and G. Marchesini, Phys. Rep. vol. 100, n.4 (1983), 201.
- (30) L.V. Gribov, E.M. Levin and M.G. Ryskin, Physic Report 100 (1983) 1.
- (31) M. Froissant, Phys. Rev. 123 (1961) 1053.
- (32) J. Kuti and V.F. Weisskopf, Phys. Rev. D4 (1971) 3418.
- (33) R.W. Brown and K.O. Michaelian, Phys. Rev. D19 (1979) 922;
R.W. Brown, D. Sahdev and K.O. Michaelian, Phys. Rev. D20 (1979) 1164. R.W. Brown, Fermilab Conf-82117-THY (Feb. 1982).
- (34) C. Goebel, D.M. Scott and F. Halzen, Phys. Rev. D22, 2789 (1980).

- (35) S.D. Drell and T.M. Yan, Phys. Rev. Lett. 25, 316 (1970) and Ann. Phys. (NY) 66, 578 (1971).
- (36) G. Altarelli, G. Parisi and R. Petronzio, Phys. Lett. 76B, 351 (1978) and Phys. Lett. 76B, 356 (1978).
- (37) H.D. Politzer, Nucl. Phys. B129, 301 (1977).
- (38) C.T. Sachrajda, Phys. Lett. 73B, 185 (1978).
- (39) F. Halzen and D. Scott, Phys. Rev. D18, 3378 (1978) and Phys. Rev. D19, 216 (1979).
- (40) H. Fritzsch and P. Minkowski, Phys. Lett. 73B, 80 (1978).
- (41) K. Kajantie, J. Lindfors and R. Raitio, Phys. Lett. 74B, 384 (1978) and Nucl. Phys. B144, 422 (1978).
- (42) R.D. Field, Lectures at the La Jolla Institute Summer Workshop (1978), Caltech preprint CALT-68-696.
- (43) G. 't Hooft, Nucl Phys. B72 (1974) 461.